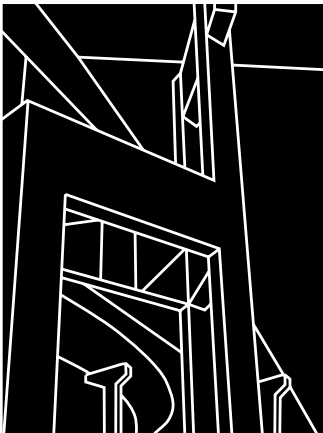


RESEARCH REPORT 1814-2

REPORT ON THE FIRST JACKSBORO MMLS TESTS

André de Fortier Smit, Fred Hugo, and Amy Epps



CENTER FOR TRANSPORTATION RESEARCH
BUREAU OF ENGINEERING RESEARCH
THE UNIVERSITY OF TEXAS AT AUSTIN

DECEMBER 1999

1. Report No. FHWA/TX-00/0-1814-2	2. Government Accession No.	3. Recipient's Catalog No.	
4. Title and Subtitle REPORT ON THE FIRST JACKSBORO MMLS TESTS		5. Report Date December 1999	
7. Author(s) André de Fortier Smit, Fred Hugo, and Amy Epps		6. Performing Organization Code	
		8. Performing Organization Report No. 0-1814-2	
9. Performing Organization Name and Address Center for Transportation Research The University of Texas at Austin 3208 Red River, Suite 200 Austin, TX 78705-2650		10. Work Unit No. (TRAIS)	
		11. Contract or Grant No. 0-1814	
12. Sponsoring Agency Name and Address Texas Department of Transportation Research and Technology Transfer Section/Construction Division P.O. Box 5080 Austin, TX 78763-5080		13. Type of Report and Period Covered Research Report (9/1/98 to 8/31/99)	
		14. Sponsoring Agency Code	
15. Supplementary Notes Project conducted in cooperation with the U.S. Department of Transportation, Federal Highway Administration, and the Texas Department of Transportation.			
16. Abstract <p>This report outlines the two accelerated pavement tests completed in Jacksboro, Texas, using the 1/3-scale Model Mobile Load Simulator (MMLS3). The MMLS3 tests were initially commissioned to investigate the stripping phenomenon evident under conventional trafficking of the outside lane adjacent to the TxMLS testing in the region. To achieve this goal, the MMLS3 was used in the field to test a pavement section on the northbound carriageway of US 281 near Jacksboro. During trafficking of the first MMLS3 test, water flowed over the pavement surface to accelerate the effects of stripping. Subsequent testing with the MMLS3 was used to investigate and compare the relative rutting of the 1/3-scale machine to that of the full-scale TxMLS without the use of water.</p> <p>In addition to the technical goals described, further development of the prototype MMLS3 was of particular interest. The mean combined operational productivity of the MMLS3 for the wet and dry tests was 79 percent, 13 percent, and 8 percent for run, maintenance, and data collection time, respectively. For both the wet and dry tests, data collection included hourly asphalt layer temperature monitoring, frequent transverse surface profiling, Surface Analysis of Spectral Waves (SASW) analyses, and relative asphalt surface deformation measurements.</p> <p>It was found that the temperature gradient of the asphalt concrete layer with water flowing over the surface (the wet test) ranged from 24 °C to 27 °C. For the dry test, the gradient ranged from 33 °C to 38 °C. The SASW modulus ratios (trafficked versus control sections) determined at the termination of the wet and dry MMLS3 tests were 38 percent and 90 percent, respectively, indicating that the asphalt surfacing (overlay) on the northbound carriageway of US 281 is potentially susceptible to moisture damage. For this reason, additional wet MMLS3 testing is recommended on the southbound carriageway of US 281 to ascertain whether this overlay is also susceptible, given that it performed relatively well under dry conditions.</p>			
17. Key Words: Texas Mobile Load Simulator, accelerated pavement testing		18. Distribution Statement No restrictions. This document is available to the public through the National Technical Information Service, Springfield, Virginia 22161.	
19. Security Classif. (of report) Unclassified	20. Security Classif. (of this page) Unclassified	21. No. of pages 64	22. Price

REPORT ON THE FIRST JACKSBORO MMLS TESTS

by

André de Fortier Smit
Fred Hugo
Amy Epps

Research Report Number 1814-2

Research Project 0-1814
Project Title: MLS Research Management System — Phase II

Conducted for the

TEXAS DEPARTMENT OF TRANSPORTATION

in cooperation with the

**U.S. DEPARTMENT OF TRANSPORTATION
FEDERAL HIGHWAY ADMINISTRATION**

by the

CENTER FOR TRANSPORTATION RESEARCH
Bureau of Engineering Research
THE UNIVERSITY OF TEXAS AT AUSTIN

and the

**TEXAS TRANSPORTATION INSTITUTE
TEXAS A&M UNIVERSITY SYSTEM**

and

THE UNIVERSITY OF TEXAS AT EL PASO

December 1999

DISCLAIMERS

The contents of this report reflect the views of the authors, who are responsible for the facts and the accuracy of the data presented herein. The contents do not necessarily reflect the official views or policies of either the Federal Highway Administration (FHWA) or the Texas Department of Transportation (TxDOT). This report does not constitute a standard, specification, or regulation.

There was no invention or discovery conceived or first actually reduced to practice in the course of or under this contract, including any art, method, process, machine, manufacture, design or composition of matter, or any new and useful improvement thereof, or any variety of plant, which is or may be patentable under the patent laws of the United States of America or any foreign country.

NOT INTENDED FOR CONSTRUCTION, BIDDING, OR PERMIT PURPOSES

Frederick Hugo, P.E. (Texas No. 67246)
Research Supervisor

Research performed in cooperation with the Texas Department of Transportation and the U.S. Department of Transportation, Federal Highway Administration.

ACKNOWLEDGMENTS

The researchers appreciate the assistance provided by Mr. Ken Fults, P.E. (DES), who served as the project director for this research effort until he was succeeded by Dr. Mike Murphy, P.E. (DES). Research was performed in cooperation with TxDOT. The authors also wish to extend thanks to the following individuals for assistance provided during the MMLS3 tests in Jacksboro:

TxDOT: Ken Fults, Dr. Mike Murphy, Mike Finger, Sherwood Helms, Dr. Dar-Hao Chen,
and John Bilyeu

TxMLS Team 1: John Earl Barrett, Terry Ludwig, Cody Smith, and Patrick Ball

TxMLS Team 2: Sam Ragsdill, Lance Broussard, Ron Broussard, and Mitchell Corliss

TTI: Dr. Dallas Little, Rajesh Bhairampally, and Gene Schlieker

CTR: Dr. Joe Allen

Others: Bob Sieberg and Doug Adams

TABLE OF CONTENTS

1. INTRODUCTION.....	1
2. MMLS3 TEST SETUP AND METHODOLOGY.....	2
3. MMLS3 PRODUCTIVITY	5
4. DATA COLLECTION.....	6
5. RESULTS.....	7
5.1 TEMPERATURE PROFILES	7
5.2 RUTTING RESULTS.....	9
5.3 SASW MODULUS RESULTS.....	13
5.4 CRACKING OBSERVED ON THE WET TEST PAVEMENT	14
6. DISCUSSION	15
6.1 MODEL TESTING IN THE FIELD.....	15
6.2 STRESS/STRAIN ANALYSES	15
6.3 EVALUATION OF THE RUTTING PERFORMANCE.....	17
6.4 EVALUATION OF THE SASW YOUNG’S MODULUS RESULTS.....	18
6.5 MATERIAL CHARACTERIZATION.....	18
7. CONCLUSIONS.....	22
8. RECOMMENDATIONS	22
REFERENCES.....	25
APPENDIX A: INITIAL DIAGNOSTIC INTERPRETATION OF THE PERFORMANCE OF MLS TEST PAD SI IN JACKSBORO.....	27
APPENDIX B: NOTES ON OPERATING THE MMLS3 PROTOTYPE	45

LIST OF FIGURES

Figure 1. US 281 northbound carriageway pavement structures	2
Figure 2. MMLS3 test grid.....	3
Figure 3. Closed-loop water system used for wet MMLS3 tests	3
Figure 4. Layer deformation measurement gauge and installation	4
Figure 5. Wet test total time breakdown and operational productivity charts	5
Figure 6. Dry test total time breakdown and operational productivity charts.....	6
Figure 7. Profilometer measurements on MMLS3 test grid.....	6
Figure 8. SASW measurements and data collection	7
Figure 9. Wet test asphalt layer temperature variation with MMLS3 trafficking.....	7
Figure 10. Wet daily asphalt layer temperature variation	8
Figure 11. Dry test asphalt layer temperature variation with MMLS3 trafficking	8
Figure 12. Dry test daily asphalt layer temperature variation	9
Figure 13. Wet test cumulative maximum rutting	10
Figure 14. Wet test 8 (0.8 m) grid line transverse surface deformation with trafficking.....	10
Figure 15. Dry test cumulative maximum rutting.....	11
Figure 16. Dry test 10 (1 m) grid line transverse surface deformation with trafficking	11
Figure 17. TxMLS vs. MMLS3 rutting (left wheelpath of northbound US 281)	12
Figure 18. Relationship between TxMLS and MMLS3 rutting	12
Figure 19. Wet and dry test SASW modulus change with MMLS3 trafficking	13
Figure 20. SASW modulus change with TxMLS trafficking.....	14
Figure 21. Surface cracking observed after the wet test	14
Figure 22. (a) and (b) Model tests in the field for (a) uniform material and (b) composite layered structure	16
Figure 23. (a) and (b). Elastic stress distribution with depth for TxMLS and MMLS3 tests	17

LIST OF TABLES

Table 1. Wet and dry test SASW Young's modulus results	13
Table 2. Moisture sensitivity results at 25 °C (AASHTO T283).....	19
Table 3. Volumetric results	19
Table 4. Average SST frequency sweep results @ 2 Hz, 5 Hz, and 10 Hz	20
Table 5. Average SST RSST-CH results at 40 °C	21

ABSTRACT

This report outlines two accelerated pavement tests completed on US 281 in Jacksboro, Texas, using the 1/3-scale Model Mobile Load Simulator (MMLS3). The MMLS3 tests were initially commissioned to investigate the stripping phenomenon evident under conventional trafficking of the outside lane adjacent to the TxMLS testing in the region. To achieve this goal, the MMLS3 was used in the field to test a pavement section on the northbound carriageway of US 281 near Jacksboro. (This section had been rehabilitated with Dustrol.) During trafficking of the first MMLS3 test, water flowed over the pavement surface to accelerate the effects of stripping. Subsequent testing with the MMLS3 was used to investigate and compare the relative rutting of the 1/3-scale machine to that of the full-scale TxMLS without the use of water.

In addition to the technical goals described, further development of the prototype MMLS3 was of particular interest. The mean combined operational productivity of the MMLS3 for the wet and dry tests was 79 percent, 13 percent, and 8 percent for run, maintenance, and data collection time, respectively.

It was found that the temperature gradient of the asphalt concrete layer with water flowing over the surface (the wet test) ranged from 24 °C to 27 °C (75 °F to 80.6 °F). For the dry test, the gradient ranged from 33 °C to 38 °C (91.4 °F to 100.4 °F).

The Surface Analysis of Spectral Waves (SASW) modulus ratios (trafficked versus control sections) determined at the termination of the wet and dry MMLS3 tests were 38 percent and 90 percent, respectively, indicating that the asphalt mixes of the rehab process on the northbound carriageway of US 281 are potentially susceptible to moisture damage. For this reason, additional wet MMLS3 testing is recommended on the southbound carriageway of US 281 to ascertain whether its Remixer rehab is also susceptible, given that it performed relatively well under dry conditions.

Surface microcracking was evident in the wheelpath of the MMLS3 after termination of the wet test. This microcracking suggests that the surface layer underwent degradation as a result of the effect of trafficking on water. The extent and nature of this distress must still be identified by coring and by subsequent strength and fatigue testing.

Rutting was the anticipated mode of pavement failure for the dry test. Based on transverse surface profiles, the maximum rut depth at the termination of this test after the application of 1 million MMLS3 loads was 1.8 mm ± 0.2 mm (0.07 in. ± 0.01 in.). This permanent deformation occurred in the upper 90 mm (3.55 in.) of the asphalt concrete layer. The maximum rut depth in the wet test was approximately 1 mm (0.04 in.). The rutting measured during the MMLS3 test was compared to that observed under TxMLS loading in the left wheelpath of the inner lane of the northbound carriageway of US 281. Up to 100,000 load applications, the rut depths compare well, with the rut under TxMLS loading approximately 2.9 times the MMLS3 rut depth. After 80,000 load applications, the rate of rutting under the TxMLS became much higher than that under the MMLS3, probably as a result of shear failure of either the upper surfacing asphalt concrete layer or underlying lightweight aggregate layer. To investigate the difference in rutting between the TxMLS and

MMLS3, it is recommended that additional MMLS3 tests be performed in Jacksboro as a next phase. These tests should be undertaken directly on the lightweight aggregate layer by milling off the upper 25 mm (0.98 in.) of the asphalt concrete surfacing. This will allow a higher stress level under the MMLS3 deeper within the asphalt concrete layer and will indicate which of the asphalt concrete layers is most susceptible to shear failure.

A limited laboratory testing program was completed to further explore the pavement distress observed under the MMLS3 trafficking. From the results of these tests, further evidence was found that the surface layers are susceptible to stripping. High shear stiffness values and RSST-CH results indicate that the upper layers of the pavement are relatively resistant to permanent deformation. The small rut depths measured under the MMLS3 correlate with these findings.

It is recommended that cores be taken inside the wheelpaths of the wet and dry MMLS3 test sections. Laboratory testing of these cores should be performed to ascertain:

- the extent and nature of the surface distress apparent on the wet test pad, with particular attention to the stripping potential of the respective layers;
- the resistance to shear failure of the asphalt concrete layers on the dry test pad; and
- fatigue performance of the respective sections (this performance should be compared with that of untrafficked sections).

1. INTRODUCTION

Conventional trafficking of the outside lane adjacent to the TxMLS testing and subsequent full-scale TxMLS tests provided evidence of stripping of the layer of lightweight aggregate asphalt concrete (LWAC) underlying the Remix rehabilitation surfacing on the southbound carriageway of US 281 just outside of Jacksboro, Texas (1). This stripping was found in an initial diagnostic interpretation of pavement performance of the southbound test section (S1) undertaken in 1997 (see Appendix A).

Testing with the 1/3-scale MMLS3 was approved, the goal of the tests being to investigate the stripping phenomenon by trafficking the pavement in the field with the MMLS3 with a sheet of water flowing across the pavement surface. The hypothesis was that the effect of surface water on the performance of the test pads in the northbound lane under MMLS3 trafficking would allow a better understanding of the performance of test pads N1 and S1 on US 281 under TxMLS trafficking.

Initially, additional testing was planned to investigate the extent of damage in terms of axle load and tire pressure. Initial MMLS3 testing was to be performed using a 2.1 kN* axle loading at a tire pressure of 690 kPa. This was to be followed by a test using 1.05 kN axle loading and a tire pressure of 345 kPa. The purpose of the second set of testing conditions was to maintain the depth of influence but at a reduced stress level. The hypothesis was that results from these tests would give insight into the mechanism of stripping. This additional testing was not performed; instead, another MMLS3 test under dry, warm conditions was performed alongside the wet test. The purpose of the dry test was to allow a comparison under MMLS3 trafficking and TxMLS trafficking.

This report begins by describing the test setup and the methodology followed for the wet and dry MMLS3 tests. The MMLS3 used for the tests was a prototype model, and the productivity of the machine was monitored to explore the durability of the device. This aspect is discussed briefly. Cores were taken in the vicinity of the MMLS3 test pad for material characterization, and laboratory tests scheduled for this purpose are listed.

Data collection included transverse profile measurements using the TxMLS profilometer, longitudinal and transverse SASW measurements at selected grid points, and surface deformation measurements obtained from pins installed in the pavement prior to testing. The temperature of the asphalt layer was monitored hourly from thermocouples installed and sealed at three depths (25 mm, 100 mm, and 160 mm) within the pavement structure.

The results of the wet and dry tests are reported separately, with a discussion of the results following. The anticipated modes of failure for the wet and dry tests were stripping of the lightweight aggregate asphalt concrete layer and surface rutting, respectively. The results of particular importance for the wet test are, therefore, SASW moduli measurements, evidence of stripping, and crack development. For the dry test, the surface deformation and pavement temperatures are more relevant.

A limited laboratory testing program was completed to further explore the pavement distress observed under the MMLS3 trafficking. The volumetric properties,

* Given that researchers working in the area of accelerated pavement testing (APT) use metric units, and given that TRB Task Force A2B52 on APT has set guidelines that include the exclusive use of metrics for capturing APT data, the authors have elected to use metric units exclusively in the report proper.

moisture susceptibility, stiffnesses, RSST-CH values, and strengths of cored specimens from the northbound carriageway were determined.

On the basis of a discussion of the results and conclusions, tentative recommendations for further MMLS3 testing in Jacksboro were made. Notes on the operation of the MMLS3 gathered during the tests in Jacksboro have been collected in an appendix to this report.

2. MMLS3 TEST SETUP AND METHODOLOGY

The 1/3-scale MMLS3 is a low-cost accelerated pavement testing (APT) device that applies 7,200 single-wheel applications per hour by means of a 300 mm diameter, 80 mm wide tire. Further information on the MMLS3 has been published elsewhere (2, 3). Notes on operating the MMLS3 prototype are contained in Appendix B.

For the MMLS3 test site in Jacksboro, it was necessary to select near the TxMLS test site a flat area of suitable size having reasonably uniform material properties. A section south of the current TxMLS test pad (Pad N1) on the northbound carriageway of US 281 was selected based on SASW and falling weight deflectometer (FWD) test results that had been completed on this section to test the uniformity of the site area for the TxMLS tests. The chosen site fell between the thermal cracks on this section. Figure 1 shows the pavement structure for the northbound carriageway.

A test grid (see Figure 2) was painted on the pavement in line with the right and left wheelpaths on the TxMLS test pad for the wet and dry MMLS3 tests, respectively. The grid was marked for the profilometer readings and the SASW positions. Profilometer guide rails were installed on the pavement. A water system consisting of a water pump, sump pump, hose pipes, perforated pipe, and connectors was set up to control the flow of water across the test pad for the wet MMLS3 tests. The plan view schematic shown in Figure 3 details the closed-loop system used. The setup was such that the water flowed across the test pad at a rate of approximately 600 litres/hour, resulting in a 1 mm thick water layer equivalent to rain falling at 5 mm/hour. A hole to hold the sump pump was cored in the lowest level of the test area and sealed. The test area was sealed to prevent the flow of water into oncoming traffic lanes.

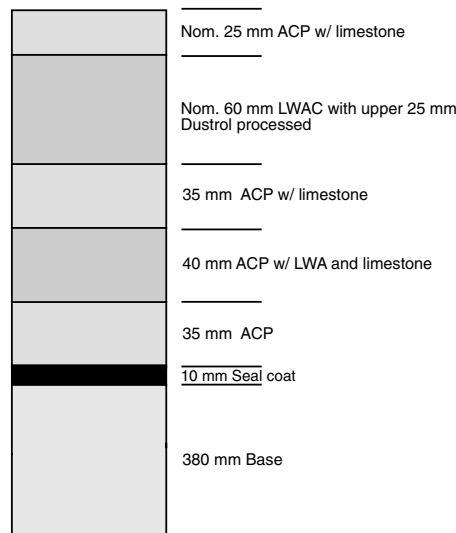


Figure 1. US 281 northbound carriageway pavement structures

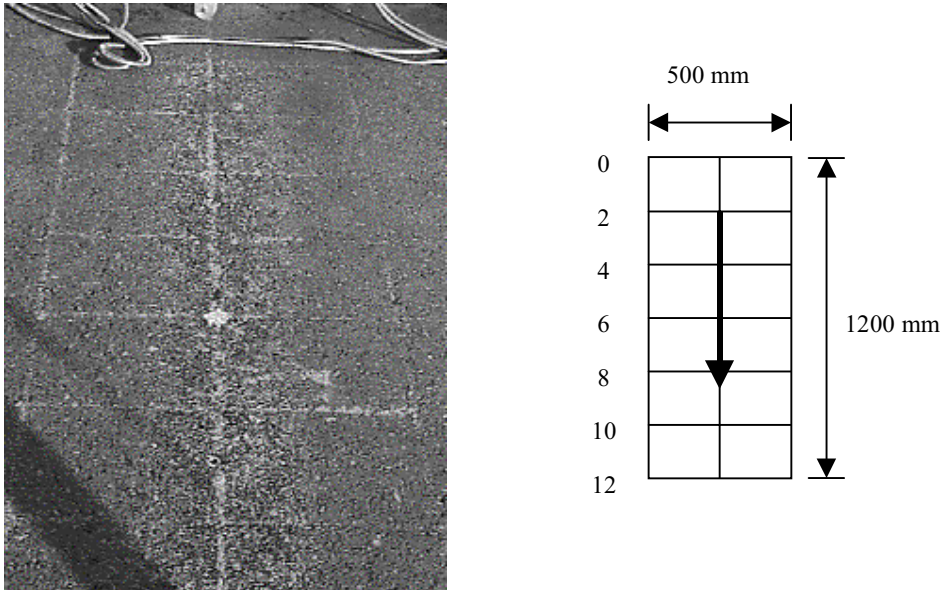


Figure 2. MMLS3 test grid

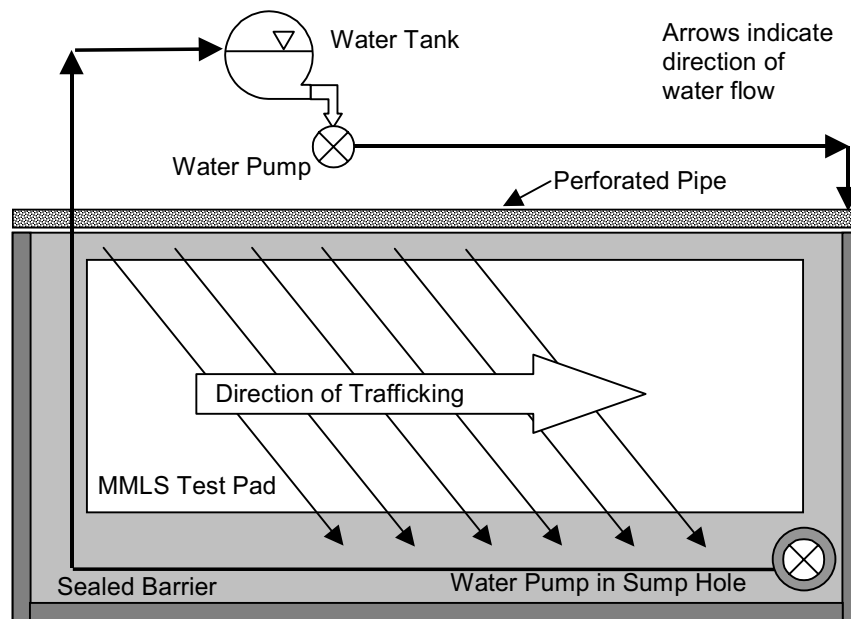


Figure 3. Closed-loop water system used for wet MMLS3 tests

Deformation pins were installed at two locations (0.3 m and 0.9 m) on the center grid line to measure the relative deformation of the surface layer with MMLS3 trafficking.

Figure 4 shows the deformation measurement gauge used to measure the relative deformation of the asphalt concrete surface layer. The gauge measures the distance to the top of a pin installed at a depth of 90 mm within the asphalt concrete layer, as shown in the figure.

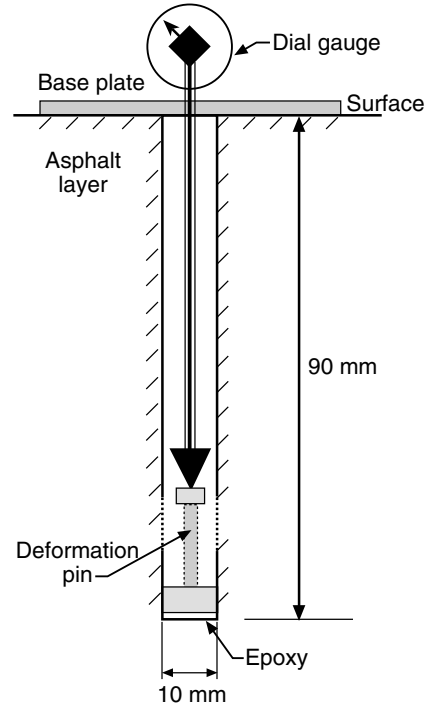
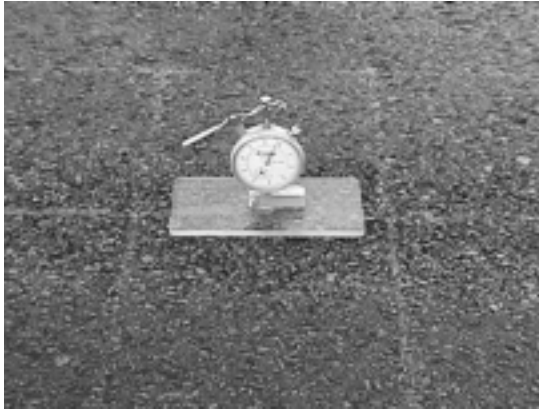


Figure 4. Layer deformation measurement gauge and installation

A thermocouple tree was installed to monitor the temperature of the asphalt concrete layer at depths of 25 mm, 100 mm, and 160 mm. Cores were taken in and between the wheelpaths from the test pavement in the vicinity of the MMLS3 test pad for material characterization by the Texas Transportation Institute (TTI). A range of laboratory tests have been completed, including the following:

- Volumetric characterization: determination of bulk relative density, voids in the mix (VIM), and voids in the mineral aggregate (VMA)
- Moisture susceptibility: American Association of State Highway and Transportation Officials (AASHTO) T283 test method
- Repeated shear tests at constant height at 40 °C and a shear stress level of 68 kPa
- Frequency sweep tests at frequencies ranging from 0.1 to 10 Hz and test temperatures of 25 °C and 40 °C

Laboratory testing was conducted on two types of cylindrical specimens cut from field cores taken adjacent to the MMLS3 test pads. Composite specimens consisted of the upper 50 mm of the pavement structure, including some of the surface overlay and some of the lightweight aggregate asphalt concrete. The second type of specimen consisted of only the material in the layer containing lightweight aggregate.

NOTE: Additional ITS and fatigue tests were performed on cores obtained from the wet and dry MMLS3 section. The results of these tests are reported and discussed in Research Report 1814-3, which documents the next phase of MMLS testing.

3. MMLS3 PRODUCTIVITY

The procedure followed for the MMLS3 tests was similar to that followed for the wet and dry tests in that after a specific number of axles had been applied, the MMLS3 was removed from the test pad, data were collected, and the procedure was repeated. The wet test was run continuously 24 hours a day from 19 August until 3 September 1998, a period of 16 days, with the test interrupted only to collect data and to respond to mechanical breakdowns. During this time, a total of 1.45 million MMLS3 axles were applied to the pavement. Water was allowed to flow over the test pavement during testing. The dry test was run from 8 September until 1 October, a period of 24 days. The dry test axle application was performed during those hours of the day when the upper 25 mm of the asphalt surfacing was above 30 °C, typically between 10:00 and 20:00 during the day. This temperature condition is conducive to rutting of this layer, which was the anticipated mode of failure for this test. The dry test was terminated after 1 million load applications.

Figure 5 and Figure 6 show the breakdown of time and productivity during the wet and dry test periods, respectively. The figures break down the test period into time running (traffic), data collection, maintenance to the MMLS3, and nonoperational time. The data collection process is discussed in the next section. Maintenance included repair to the machine and time wasted waiting for spare parts. Nonoperational time is defined as that time during the test period when the machine was intentionally not operating. This time included weekend breaks and intervals when the temperature of the upper 25 mm of the asphalt layer was lower than 30 °C for the dry tests. The productivity charts shown on the right side of the figures do not include nonoperational time to allow a more realistic evaluation of the time breakdown during operational hours. From these figures it can be seen that the run time for the wet and dry tests is approximately 80 percent of the operational time. The relatively high maintenance time for the wet test was mainly due to design and manufacturing faults on the prototype that have subsequently been corrected. It should be noted that the maintenance time for the dry test was 12 percent of the operational time. This seemingly excessive percentage, which distorts the productivity reported during this test, was a result of having to replace a fused electronic controller; this replacement required a 2-day wait for the new controller to arrive on site. Aside from this delay, the MMLS3 ran faultlessly throughout the dry test.

Period: 19 August - 3 September

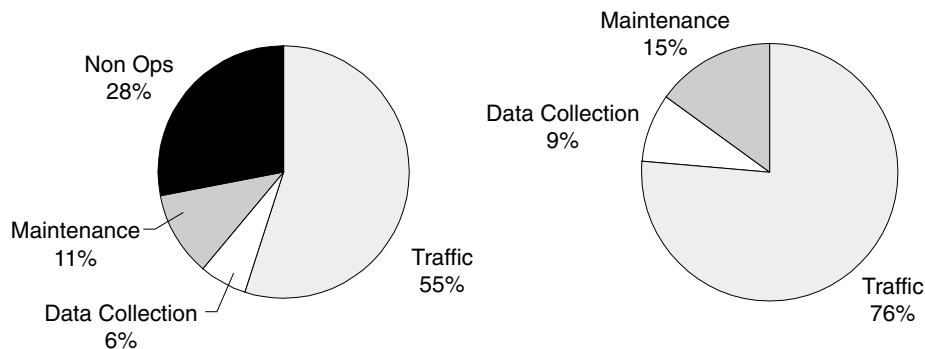


Figure 5. Wet test total time breakdown and operational productivity charts

Period: 8 September - 1 October

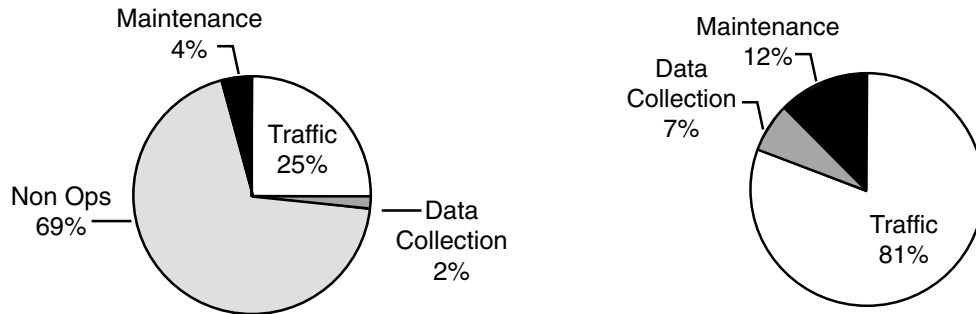


Figure 6. Dry test total time breakdown and operational productivity charts

In summary, the mean combined operational productivity of the MMLS3 for the wet and dry tests was 79 percent, 13 percent, and 8 percent for run, maintenance, and data collection time, respectively.

4. DATA COLLECTION

Data collection included seven transverse surface profile measurements along the test grid using the TxMLS profilometer (see Figure 7). The profilometer measures changes in height relative to a position that is given fixed coordinates (the lower right point on the test grid).

SASW measurements (see Figure 8) were made at fourteen longitudinal and three transverse positions along the test grid. The grid positions, 250 mm left from the trafficking line, or centerline, were used as control points. Two different sensor spacings of 150 mm and 100 mm were used. Some of the SASW measurements were performed directly beneath the MMLS3 without having to remove it from the test pad. The surface temperature of the pavement was monitored for the duration of the SASW tests.

Temperatures were monitored hourly before and during MMLS3 testing at three depths (25 mm, 100 mm, and 160 mm) within the asphalt layer.



Figure 7. Profilometer measurements on MMLS3 test grid

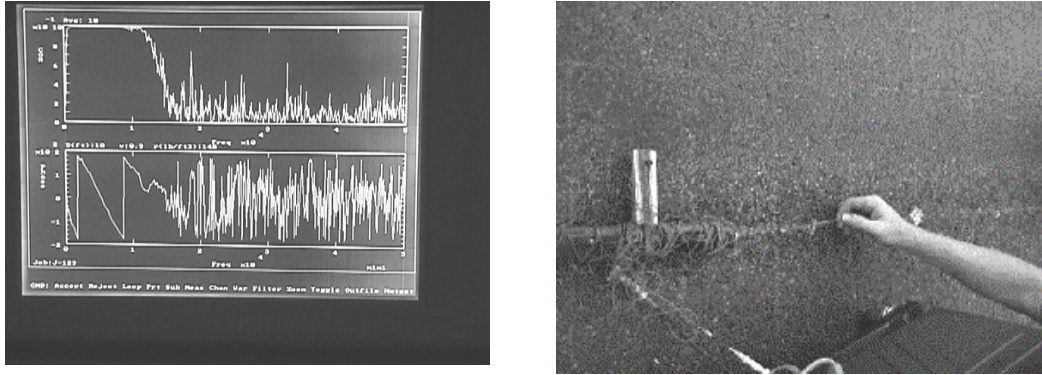


Figure 8. SASW measurements and data collection

5. RESULTS

This section presents a summary of the results collected during the wet and dry MMLS3 tests.

5.1 Temperature Profiles

5.1.1 Temperature profiles during the wet test: Figure 9 shows the temperature variation at three depths (25 mm, 100 mm, and 160 mm) within the asphalt concrete layer for the duration of the wet test. The gap in the data indicates the point at which the temperature probe was down. It can be seen that the temperature profile in the asphalt layer is top low and bottom high. The mean temperature at the 25 mm depth was about 24 °C and, at the 160 mm depth, 27 °C. The temperature in each section of the asphalt concrete layer remained fairly constant, with little variation occurring throughout the test. A gradual decrease in temperature with trafficking is evident with the approach of the fall season. Figure 10 shows the typical daily temperature profile in the asphalt layer. Polynomial trendlines have been fitted through the data to emphasize the daily cyclic variation. As expected, the greater variation is in the upper section of the asphalt layer. Outliers are evident in the temperature data taken at the 25 mm depth. This could be related to the periods when profilometer and SASW measurements were taken. During these periods the surface was dried, allowing the surface to heat.

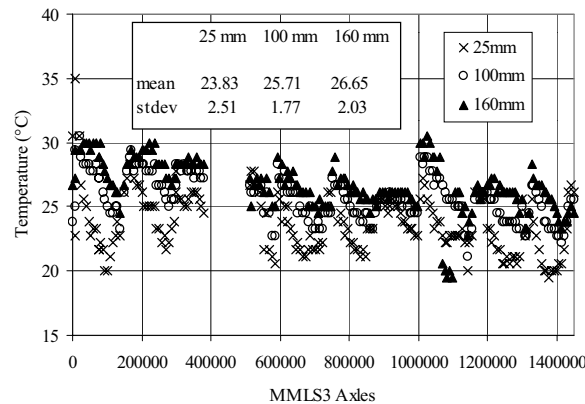


Figure 9. Wet test asphalt layer temperature variation with MMLS3 trafficking

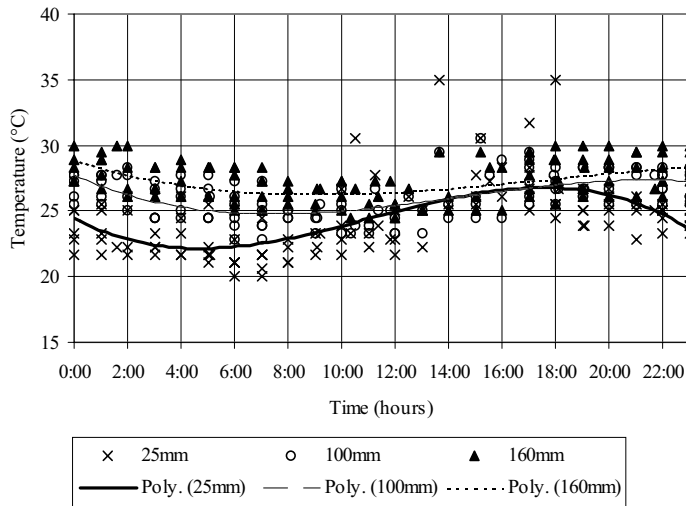


Figure 10. Wet daily asphalt layer temperature variation

5.1.2 *Temperature profiles during the dry test:* Figure 11 shows the temperature profile in the asphalt concrete layer during the dry MMLS3 test. The mean temperature in any asphalt layer was above 30 °C — and closer to 40 °C — in the upper 25 mm of the asphalt layer. The temperatures remained fairly constant with trafficking, the standard deviation being about 5 °C in the upper 25 mm of the asphalt. Figure 12 shows the typical temperature profiles between 9:00 and 21:00 during the dry MMLS3 tests. As expected, the maximum temperature at each of the temperature probe levels occurs at different times during the day.

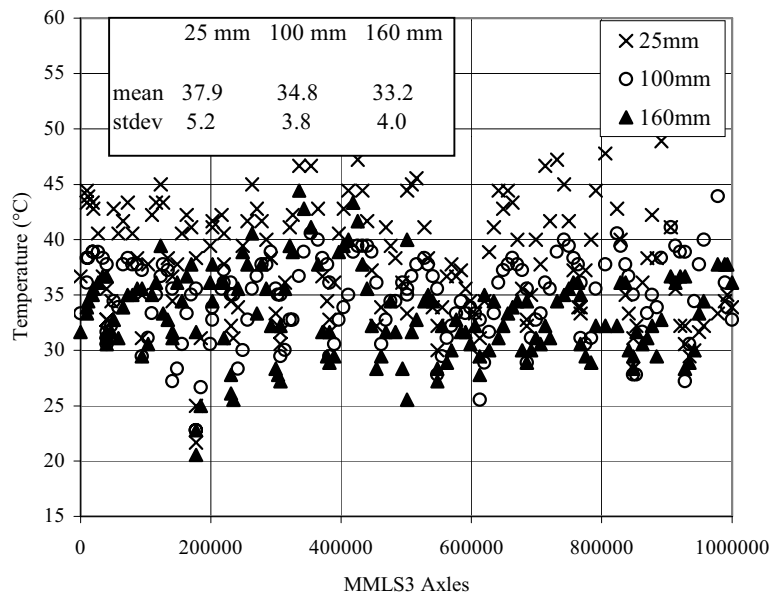


Figure 11. Dry test asphalt layer temperature variation with MMLS3 trafficking

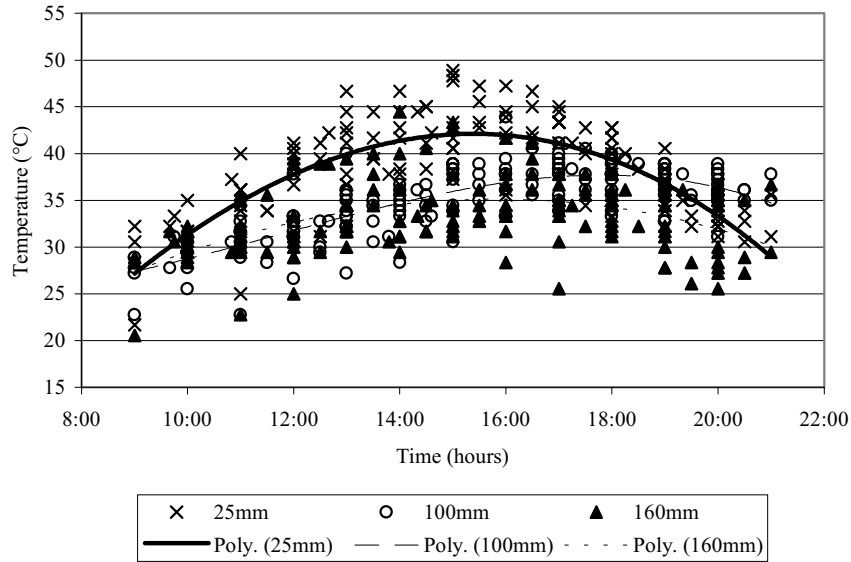


Figure 12. Dry test daily asphalt layer temperature variation

5.2 Rutting Results

The maximum rut depths given in this report were determined by applying an imaginary straightedge over the maximum surface elevations and calculating the vertical distance to the lowest surface elevation. While the profilometer measures accurately to 0.025 mm, the horizontal location of the plunger on the x-axis during measurements of the profiles had a window of almost 10 mm. As a result, the measuring error during the cold test was found to be +/-0.125 mm. This error was evident in the rutting data (as will be discussed subsequently) and should be taken into account in evaluating the rut profiles. Another factor to consider is the wander pattern applied to the MMLS3 wheels during trafficking. This pattern is triangular in shape and has a base width of 150 mm. The same applies to the relative deformation of the upper 90 mm of the asphalt concrete layer, as measured using the deformation pins (discussed below).

5.2.1 Rutting results for the wet test: It should be pointed out that microfracturing and not rutting was the anticipated pavement failure criterion for the wet test. Figure 13 shows the cumulative maximum rutting of the wet test pavement with MMLS3 trafficking. The rut depths at selected transverse grid points are shown and averaged in the figure. The selected grid points were in the middle of the test pad and, for this reason, had the most uniform loading. It can be seen that the pavement rutted early: 0.5 mm within 10,000 load applications. Thereafter, the rutting rate reduced continuously up to the completion of the test. It is, however, important to note that a careful review of the transverse profiles at gridlines 4 and 6 after 1450k axles indicated that the MMLS may have shifted off line at the zero end during trafficking of the last 150k axles. This apparently caused a slight upward shove on the proper centerline. The net result was an apparent decrease in the rut depth after the last 150k axle applications. This response can be seen in Figure 13 showing the rut vs. axle profile for the duration of the test. The mean rut at the end of the test, was taken to be 1 +/- 0.2 mm. The transverse surface profile at

the 8 (0.8 m) grid point is shown in Figure 14. At this small rutting level, the resolution of the profilometer is such that the rut profile is not clearly defined.

The total mean relative deformation of the upper 90 mm of the asphalt concrete layer (measured using the deformation pins) at the termination of the wet test was measured as 0.83 mm. This measurement indicates that the majority of the rutting took place in the upper 90 mm of the asphalt layer as expected.

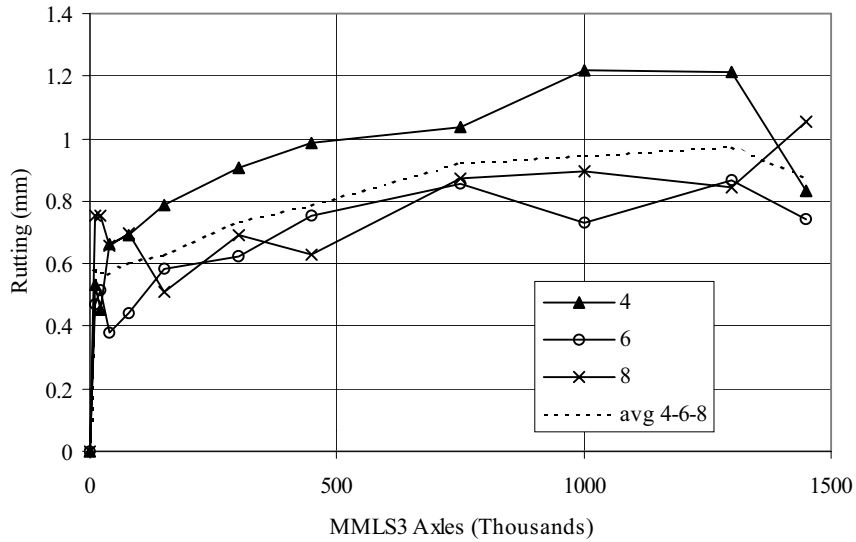


Figure 13. Wet test cumulative maximum rutting

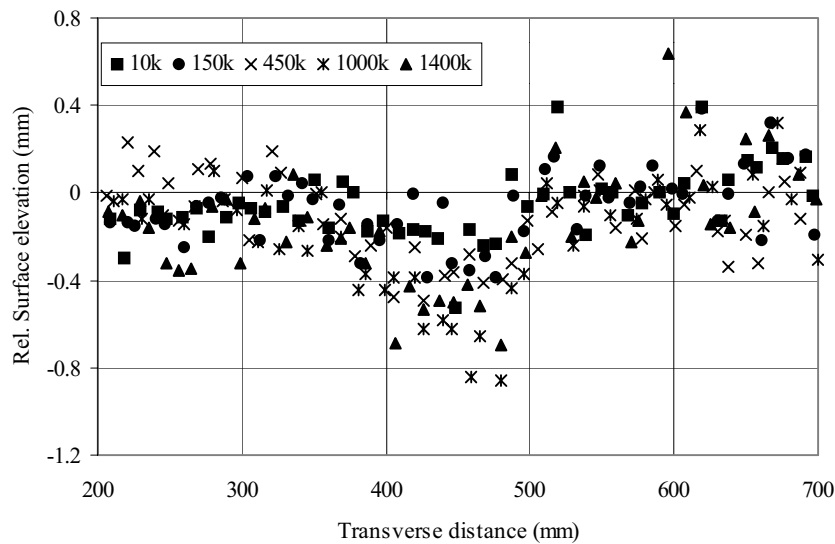


Figure 14. Wet test 8 (0.8 m) grid line transverse surface deformation with trafficking

5.2.2 *Rutting results for the dry test:* For the dry test, rutting was the anticipated mode of pavement failure — a failure promoted by the high pavement temperatures (see Figure 11) during this test. Figure 15 shows the dry test maximum cumulative rut depth with trafficking. The rut depths at selected grid points straddled around the middle of the test pad have been averaged and a logarithmic trend line superimposed. The variation between the rut depths at the selected grid points is small. The total rutting at the termination of the test (after 1 million load applications) was approximately 1.8 ± 0.2 mm. Figure 16 shows the surface elevations at the No. 10 (1 m) grid point with trafficking. From this figure, it is clear that the larger rut is more clearly defined than the rut in the wet test.

The total mean relative deformation of the upper 90 mm of the asphalt concrete layer (measured using the deformation pins) at the termination of the dry test was measured as 1.8 mm. This measurement indicates that all of the surface rutting occurred in the upper 90 mm of the asphalt concrete layer as expected.

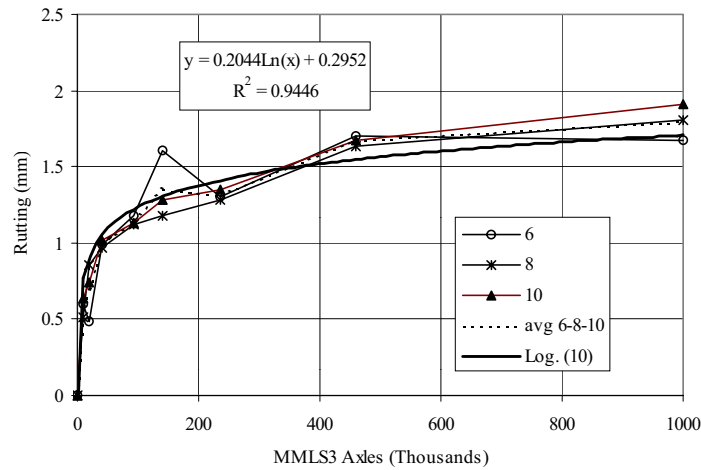


Figure 15. Dry test cumulative maximum rutting

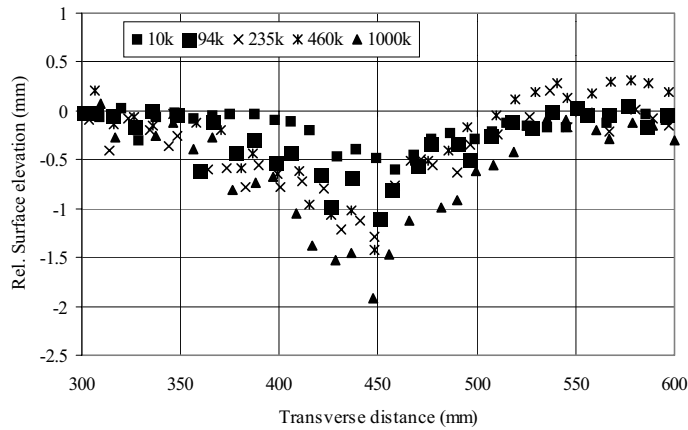


Figure 16. Dry test 10 (1m) grid line transverse surface deformation with trafficking

5.2.3 Comparing the full-scale TxMLS and MMLS3 rutting: One of the objectives of the dry test was to compare the relative rutting obtained from the TxMLS and MMLS3 tests. The MMLS3 test was performed on the left wheelpath of the interior lane of northbound US 281. The TxMLS rutting in this same wheelpath is compared in Figure 17 up until 600,000 load applications (the number of TxMLS load applications completed at the time of comparison). Figure 18 shows the relationship among the rut depths. From these figures, it is clear that the rate of TxMLS rutting relative to the MMLS3, increased significantly after 80,000 load applications. The increased rutting in the TxMLS test is probably due to deep-seated consolidation and shear deformation of the asphalt concrete layers under the higher wheel loads. The rate of the TxMLS rutting was approximately 2.9 times greater than that of the MMLS3 up to 60,000 axles. Thereafter, the rate of the TxMLS rutting is about 12.6 times that of the MMLS3, as can be seen in Figure 18. The measured rut ratio at 600,000 axle loads was about 5. It is important to remember that these comparisons are based on raw data. In Research Report 1814-3 (10), a methodology was developed to take account of the different factors that influence the comparison.

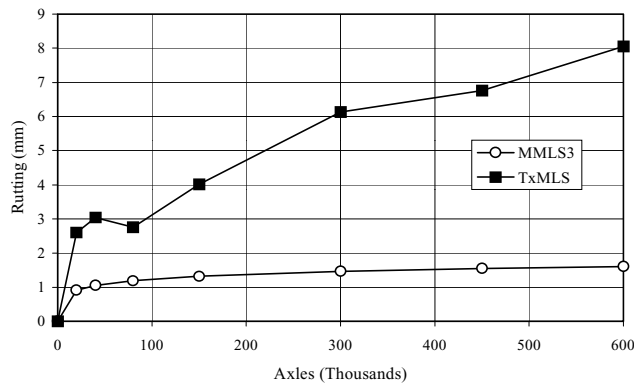


Figure 17. TxMLS vs. MMLS3 rutting (left wheelpath of northbound US 281)

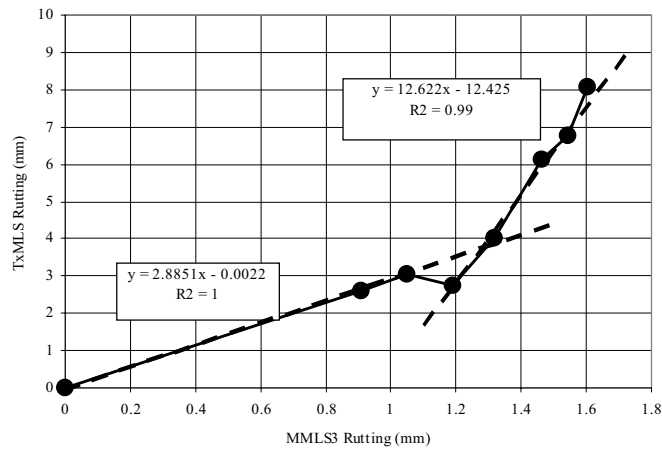


Figure 18. Relationship between TxMLS and MMLS3 rutting

5.3 SASW Modulus Results

Table 1 shows the change in the Young's modulus of the asphalt concrete surfacing with trafficking as measured using SASW for the wet and dry tests, respectively. The moduli values are given for the test and control sections before temperature correction. Dividing the test section moduli by the control section moduli results in a modulus ratio that is independent of temperature. The change in this ratio with trafficking is shown in Figure 19 for the wet and dry tests. It is immediately apparent that for the wet test, the asphalt modulus increased initially (owing to densification) and then decreased with degradation of the asphalt concrete surfacing with trafficking to 38 percent of the control section modulus. For the dry test, the modulus of the asphalt increased slightly owing to densification with trafficking. The modulus at the termination of the test was about 90 percent of that measured on the control section. This figure illustrates the effect of water on the stiffness of the asphalt concrete surfacing.

Table 1. Wet and dry test SASW Young's modulus results (30 Hz)

Wet test			Dry test		
MMLS3 Axles (Thousands)	Control section modulus (MPa)	Test section modulus (MPa)	MMLS3 Axles (Thousands)	Control section modulus (MPa)	Test section modulus (MPa)
0	4000	3800	0	3980	3047
235	3500	3700	235	5101	3839
460	3600	3500	460	5157	4417
1000	3300	2300	1000	3916	3700
1450	3200	1200			

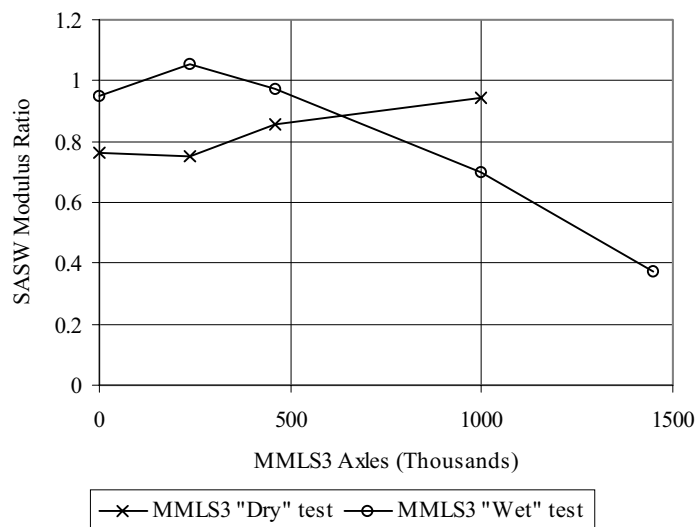


Figure 19. Wet and dry test SASW modulus change with MMLS3 trafficking

5.3.1 *Comparing the full-scale TxMLS and MMLS3 pavement moduli:* At the time of this report, the SASW wave velocities for the TxMLS pavement had been measured up to 600,000 axle repetitions. These calculations were used to determine the modulus ratios shown in Figure 20. From these results it can be seen that the moduli reductions in the left and right wheelpaths under TxMLS trafficking are similar and that the modulus after 600,000 axles is on the order of 60 percent of the control section modulus. This modulus reduction does not appear to correlate with that observed for the dry MMLS3 tests. This finding is discussed in greater detail in the next section.

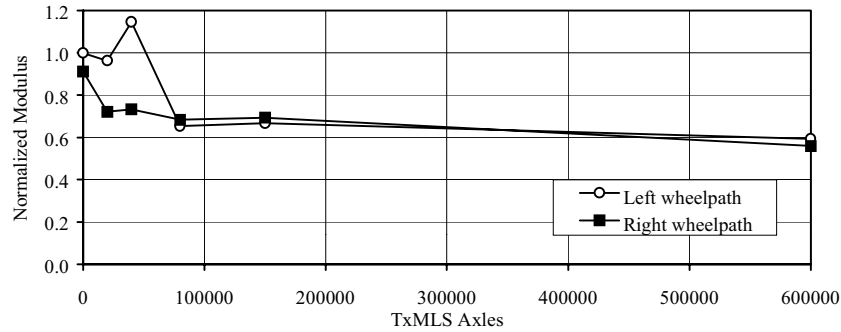


Figure 20. SASW modulus change with TxMLS trafficking

5.4 Cracking Observed on the Wet Test Pavement

Surface microcracking was observed in the MMLS3 wheelpath on the test pad after the termination of the wet test. This cracking is shown in Figure 21. The surface cracking was due to either degradation of the surface of the asphalt concrete because of the effect of water, or to stripping of the lightweight aggregate layer beneath the limestone asphalt surface. Cores were taken from the wet (and dry) test pad for laboratory testing to ascertain the extent and source of the degradation. The results of these tests are presented in Research Report 1814-3, which documents Phase II of the MMLS testing. Suffice it to say that evidence of stripping was found at the interface between the LWAC and the underlying limestone asphalt concrete.

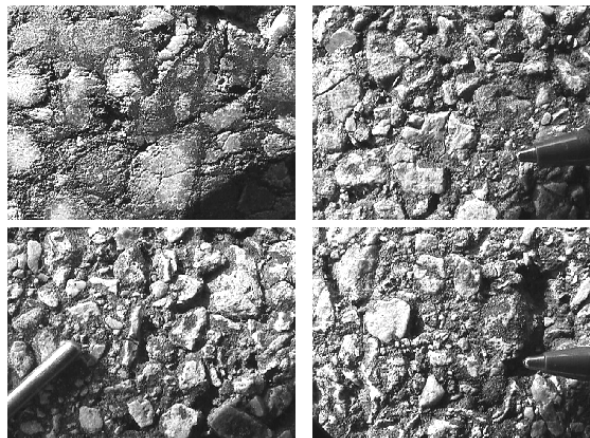


Figure 21. Surface cracking observed after the wet test

6. DISCUSSION

The discussion in this section first considers some aspects of model testing with particular reference to the use of the MMLS3 in the field. A simple stress/strain ELSYM5 (4) analysis was performed to compare the vertical stress response under both the MMLS3 and the TxMLS loads. The performance of the pavement structure under the full-scale and model loads regarding permanent deformation and stiffness loss is also discussed. Finally, results from the limited laboratory testing program are reviewed.

6.1 Model Testing in the Field

Testing a thick (i.e., 200 mm) asphalt concrete layer in the laboratory and also in the field allows application of scaling parameters based on dimensional analysis, given that a single material type is being tested. When a multilayered structure is tested, however, the situation is more complex because of the nature of the stress distribution. In addition, the materials no longer have similar characteristics, which necessitates having the layered structure scaled to satisfy dimensional analysis requirements (2). If this is not done, the scaling factor becomes inapplicable; the distress and performance then have to be related to the wheel load and stress response of the full-scale pavement structure. A marked difference in the field pavement response compared to laboratory testing was therefore to be expected in Jacksboro, Texas. The reason for this expectation is that the pavement structure is multilayered: Some layers are older than 25 years, and the rehabilitated surface layer was at least 2 years old at the time of testing. ELSYM5 (4) analyses were performed to investigate stress conditions and related performance. These analyses are discussed in the next section.

6.2 Stress/Strain Analyses

It has been shown (2) that the load amplitude of a scaled model is a square function of the scale factor relative to the full-scale load. The MMLS3 with a 2.1 kN wheel load is therefore a 1/3-scale model of the single wheel forming part of a dual wheel on a half axle having a load of 37.5 kN. The single wheel of the model therefore cannot simulate the performance under dual wheels, particularly in terms of horizontal and shear stresses. Furthermore, the stress/strain distribution within the pavement caused by the dual wheel configuration of the TxMLS will significantly differ from that under the MMLS3 single wheel load. The influence of the dual wheels of the TxMLS will be such that the vertical stresses of the individual wheels will superimpose at a specific depth (about 150 mm) within the pavement structure. The vertical stresses in the upper surfacing layer (above this point of superposition) beneath the TxMLS and MMLS3 wheel loads are, however, comparable.

A simple ELSYM5 (4) analysis allows a comparison of the elastic stress/strain distribution within the asphalt concrete pavement under TxMLS and MMLS3 loading. Using the pavement structure illustrated in Figure 1, with an asphalt concrete layer stiffness of 4,000 MPa, a base stiffness of 250 MPa, and a subgrade stiffness of 150 MPa, the stresses and strains calculated at a depth of 25 mm and at a depth below the asphalt concrete layer are shown in Figure 22. From the figure it can be seen that, although the vertical compressive stress at the surface is the same (equivalent tire pressures), the stress with depth differs. Up to a depth of 25 mm (layer thickness of the upper asphalt concrete layer), the vertical stress distribution within the asphalt concrete layer under full-scale and

MMLS3 loading is comparable, with the vertical stress at a depth of 25 mm under MMLS3 loading approximately 70 percent of that under TxMLS loading. It is obvious, however, that the horizontal strains within and below the asphalt concrete layer differ significantly under TxMLS and MMLS3 loading. It is apparent that shear stresses under the dual wheels of the TxMLS differ from those under the single wheel of the MMLS3. Furthermore, these shear stresses manifest at different positions in the transverse profile. Accordingly, the resulting shear deformation beneath the TxMLS and MMLS3 must be expected to differ.

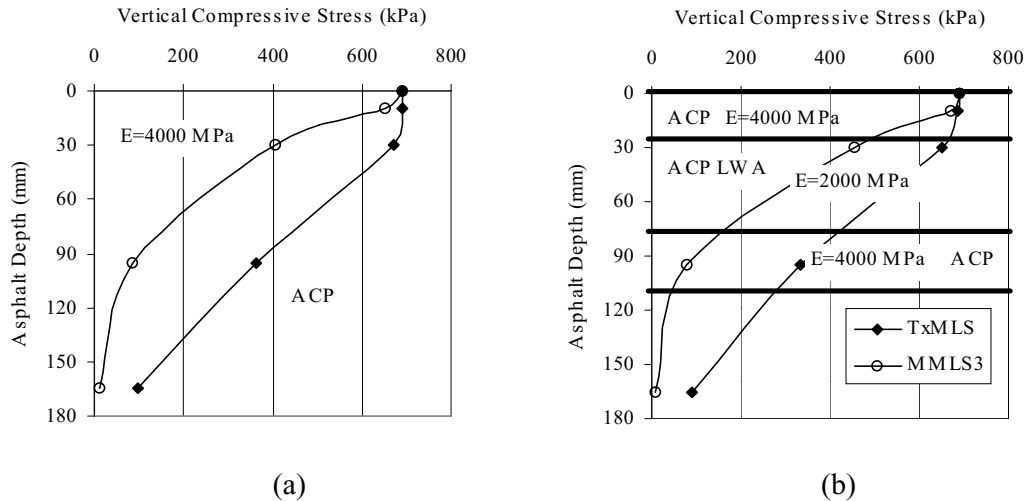


Figure 22 (a) and (b). Model tests in the field for (a) uniform material and (b) composite layered structure

Preliminary analysis of the TxMLS multidepth deflectometer (MDD) data indicates that the ratio of total deformation in the left wheelpath of the asphalt layer under TxMLS loading is 50 percent in the upper 90 mm, compared with 50 percent below that depth. As shown in Figure 17, the maximum deformation under TxMLS loading was 8 mm after 600,000 axles. Using the above ratios, the deformation in the upper 90 mm of the asphalt is 4 mm under the TxMLS, which is 2.5 times greater than the 1.6 mm maximum rut obtained under MMLS3 loading at 600,000 axles.

Figure 23 compares the vertical stress distributions within the asphalt pavement under TxMLS and MMLS3 loading. The ratio of the areas beneath the stress distribution curves for the TxMLS and MMLS3 may be directly related to the permanent deformation under the respective loads. Using this approach, the ratio of the area beneath the MMLS3 distribution compared with the TxMLS distribution is on the order of 42 percent. Applying this ratio, the permanent deformation beneath the MMLS3 should be $0.42 \times 4 \text{ mm} = 1.7 \text{ mm}$, which is very close to the 1.6 mm as measured. This result is particularly rewarding and warrants further use of the MMLS3 as a tool supplemental to the full-scale TxMLS, despite the limitations imposed by stiff pavement surfacing layers. The above reasoning is based on a limited investigation — a more detailed study of the stress distribution beneath the MMLS3 is currently underway. The performance of the test

pavements is considered in the next section in light of the analyses described. A more detailed ELSYM5 analysis was performed and is documented in Research Report 1814-3.

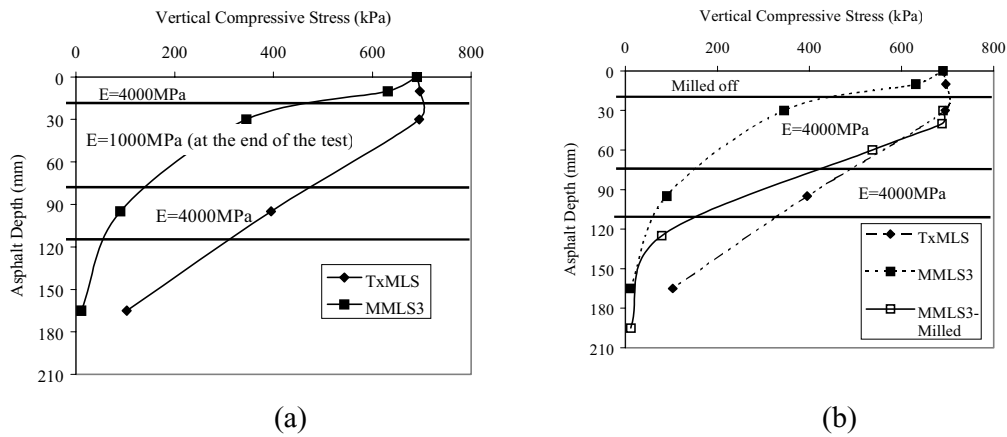


Figure 23 (a) and (b). Elastic stress distribution with depth for TxMLS and MMLS3 tests

6.3 Evaluation of the Rutting Performance

To the authors' knowledge, the MMLS3 tests in Jacksboro, Texas, were the first accelerated pavement tests performed on an in-service field pavement using a scaled-down model device for trafficking. In view of this fact it was difficult to foresee performance expectations.

As mentioned earlier, the rutting of the asphalt concrete layer under TxMLS loading was on the order of 3 times that under MMLS3 up to about 60,000 axles; thereafter, the rate of the MMLS3 rutting reduced relative to the TxMLS, causing the TxMLS ruts to be about 5 times deeper than that of the MMLS3 after 600,000 axle loads. It appears, therefore, that the rutting under the TxMLS has three mechanically different causes: consolidation, viscous flow, and shear failure (plastic flow). The viscous flow component is similar to that under the MMLS3, although the permanent deformation is greater because of the greater wheel load. The asphalt concrete layer, however, underwent plastic flow when the stresses therein exceeded the shear strength of the layer, resulting in flow of the material (or shear failure). This response was probably a result of TxMLS testing at elevated pavement temperatures and could also be due to the rehabilitation process on the northbound carriageway. The failure is evident from the shoving of the asphalt concrete in the wheelpaths under the TxMLS. Possible reasons for the difference in rutting performance between the full-scale and MMLS3 loads include the following:

1. Tire stresses: It has been shown (5) that the stresses on the edge of the tire could be as much as 3 times the tire pressure for the conventional truck tires used in the TxMLS. The stress pattern beneath the MMLS3 tires must still be defined but is expected to be very different.
2. Visco-elasto-plastic behavior of the asphalt concrete layer under TxMLS loading: The ELSYM5 calculation assumes a layered elastic pavement structure, whereas the shear failure of the asphalt concrete layer evident under TxMLS loading suggests otherwise, as will be discussed later.

3. Stress versus depth and material characteristics: Rutting of the asphalt concrete layer under the TxMLS may be due to shear failure of the lightweight aggregate layer beneath the surfacing layer of the pavement. Under full-scale loading, this layer was subjected to a much higher stress level than under MMLS3 loading.

In order to investigate the above hypotheses, it was proposed that the upper 25 mm of the limestone asphalt concrete surfacing be milled off and MMLS3 tests be done directly on the lightweight aggregate asphalt concrete layer. By doing this, greater stresses would be applied in the asphalt layer, enabling a more equitable comparison to be made between the rutting performance of the TxMLS and the MMLS3. It would allow a distinction to be made between the performance of the upper and lower asphalt layers. Figure 23(b) shows the elastic vertical compressive stress distribution beneath the MMLS3, with the upper layer milled off. At this depth, the MMLS3 can be used to apply greater stresses to the asphalt concrete layer. The results of this experiment are presented in Research Report 1814-3 (10).

6.4 Evaluation of the SASW Young's Modulus Results

The moduli reductions of the pavements on the northbound and southbound carriageways under the TxMLS were 30 percent and 14 percent (6), respectively. The modulus reduction determined under the MMLS3 on the northbound carriageway for the wet test was 62 percent. By contrast, a slight modulus increase was found for the dry MMLS3 test on the northbound carriageway. It is clear, therefore, that the modulus increase monitored on the dry MMLS3 test does not correlate with the moduli reductions on the northbound or southbound carriageways under the TxMLS. The reason for this disparity is unknown and needs to be further investigated. By contrast, however, the modulus reduction on the northbound carriageway for the wet MMLS3 tests was significantly greater than that under the TxMLS, which emphasizes the coupled effect of water and trafficking, even under the lighter load.

In light of the above, it was considered important to explore the loss of stiffness under equal stresses by performing a wet MMLS3 test on the southbound carriageway of US 281. The purpose of this test would be to determine whether the overlay strategy on the southbound carriageway is susceptible to moisture damage with trafficking and to what extent this phenomenon occurs as compared with the findings of completed TxMLS tests on the southbound carriageway and those of the TxMLS and MMLS3 tests on the northbound carriageway. The wet MMLS3 test was to be performed during the summer of 1999.

6.5 Material Characterization

The results of a limited laboratory testing program provided further evidence that the upper layers of the pavement structure are susceptible to stripping and that the underlying lightweight aggregate layer is relatively less resistant to permanent deformation. Laboratory testing was conducted on two types of cylindrical specimens (150 mm in diameter by 50 mm in height) cut from field cores taken adjacent to the MMLS3 test pads. Composite specimens (C) consisted of the upper 50 mm of the pavement structure, including some of the limestone surface overlay (approximately 25

mm) and some of the lightweight aggregate asphalt concrete (LWAC) that had been Dustrol processed. The second type of specimens (2) consisted of only lightweight aggregate nominally 45 mm thick, with the upper 25 mm Dustrol processed.

These specimens were used for moisture sensitivity testing at 25 °C (AASHTO T283) to determine the retained tensile strength ratio after wet conditioning. Shear testing using the Superpave shear tester (SST) was also performed at 25 °C and 40 °C to determine the shear stiffness (G^*) and phase angle (δ) at representative loading frequencies. The relative resistance to permanent deformation was determined using the repeated simple shear test at constant height (RSST-CH). Volumetric properties of each specimen, including air voids (VIM), voids in the mineral aggregate (VMA), and bulk specific gravity, were also determined.

6.5.1 Moisture sensitivity testing: Average moisture sensitivity test results for the composite and lightweight specimens, shown in Table 2, indicate a low level of retained tensile strength (TSR = 0.56) for the composite specimens. This level is significantly below the 0.7 or 0.8 threshold recommended in AASHTO T283 (7) and in the new TxDOT (8) and Strategic Highway Research program (SHRP) (9) procedures. The tensile strength after conditioning is also less than 800 kPa, indicating a high potential for moisture damage. The TSR of 0.82 of the LWAC is also just above the 0.8 limit. As expected, the composite layer with limestone was stronger and less ductile in indirect tension than the LWAC.

6.5.2 Volumetric properties: Average volumetric results are provided in Table 3. High VIM and VMA values were found, with the high VIM values complicating the analysis of the RSST-CH results.

6.5.3 Shear testing: The SST was used for frequency sweep testing and the RSST-CH was done at constant height. Shear frequency sweeps were conducted at 25 °C and 40 °C for composite specimens (C) and at 40 °C for lightweight specimens (L). RSST-CH tests were carried out at 40 °C at a shear stress level of 68 kPa. RSST-CH tests at 25 °C with a shear stress level of 100 kPa were discontinued during the testing program, as permanent deformation is not likely to accumulate rapidly at this temperature. A testing temperature of 40 °C is close to, but still less than, the critical temperature predicted for permanent deformation in the south-central United States (43 °C). The lower testing temperature (25 °C) is approximately the average pavement temperature at 25 mm depth for the wet test. The average pavement temperature at 25 mm depth in the dry test was between the two selected testing temperatures (38 °C).

Table 2. Moisture sensitivity results at 25 °C (AASHTO T283)

# of Specimens (Type of Specimens)	Conditioning	Indirect Tensile Strength @ Max Load	Modulus at Failure @ Max Load
2 (C)	Before (dry)	1081 kPa	268 MPa
2 (C)	After (wet)	604 kPa	159 MPa
RETAINED TENSILE STRENGTH RATIO = 0.56			

Table 3. Volumetric results

(C = Composite specimen; L = Lightweight specimen)			
# of Specimens (Type of Specimens)	Air Voids (%)	VMA (%)	BSG
12 (C)	8.6	20.1	2.022
9 (L)	9.3	22.5	1.710

6.5.4 *Frequency sweep tests:* Table 4 presents average shear frequency sweep data for representative loading times of both the TxMLS and the MMLS3. The TxMLS operates at a maximum speed of 4.9 m/sec, which corresponds approximately to a 3 Hz frequency of loading for a tread length of 250 mm based on actual measurement of a similar truck tire. The MMLS3 operates at 2.6 m/sec, which corresponds approximately to a 4 Hz frequency of loading for the smaller tire with a measured tread length of 110 mm. The results indicate that the upper surface layers and the lightweight aggregate layer are expected to behave more rigidly (with greater stiffness) under the MMLS3 (4 Hz) than under the TxMLS (3 Hz). The effect of loading time also suggests that the pavement surface layers (C) have greater resistance to permanent deformation. With the MMLS3 influencing primarily these surface layers, this result partially explains the small rut depths measured in the dry test. In comparison, the two types of specimens showed appreciable differences only in shear stiffness (G^*) and phase angle (δ) at the faster loading frequency. In addition, at the lower testing temperature the composite specimens exhibited more elastic behavior (lower δ) with higher shear stiffnesses (G^*) as expected.

Table 4. Average SST frequency sweep results @ 2 Hz, 5 Hz, and 10 Hz

(C = Composite specimen; L = Lightweight specimen)				
# of Specimens (Type of Specimens)	Temperature	Frequency (Hz)	G^* (MPa)	δ
2 (C)	40°C	2	269	42.1
		5	413	39.9
		10	534	43.3
3 (L)	40°C	2	241	41.6
		5	367	39.1
		10	700	41.6
3 (C)	25°C	2	1026	24.2
		5	1202	25.6
		10	1343	29.5

6.5.5 *RSST-CH tests:* Table 5 provides average RSST-CH results at 40 °C. These results were extrapolated to 1 percent permanent shear strain, corresponding to a 2.5 mm rut depth. Within the first 20,000 cycles, the majority of the specimens accumulated only 0.002 permanent strain. It should be noted that, because of the high resistance to permanent deformation at the selected testing temperature (40 °C), the linear extrapolation necessary to reach 1 percent (0.01) permanent strain is tenuous, as the rate of accumulation of permanent deformation may increase and the log-log relationship between permanent strain and RSST-CH repetitions may become nonlinear. The extrapolations lead to numbers of RSST-CH repetitions to only 1 percent permanent shear strain (Table 5) that are large compared with typical values. With this phenomenon in mind, the results indicate that both the composite and lightweight specimens exhibited high resistance to permanent deformation at 40 °C. This result further suggests that the surface layers of the pavement structure influenced by the MMLS3 loading are relatively

resistant to permanent deformation. Based on this finding, the rutting caused by the MMLS3 was expected to be small, as was observed in the field tests. The lightweight specimens did exhibit less resistance to rutting than did the composite specimens at 40 °C. This result helps to explain the larger rut depths measured in the TxMLS tests. The larger machine influences the lower layers of the pavement structure, including the lightweight aggregate layer, with a greater stress. This weaker layer will therefore contribute to the overall rut depth measured under the TxMLS.

Table 5. Average SST RSST-CH results at 40 °C

(C = Composite specimen; L = Lightweight specimen)		
# of Specimens (Type of Specimens)	Air voids	# RSST-CH repetitions to 1% permanent strain
2 (C)	8.4 %	4.1 E 08
2 (L)	8.1 %	1.0 E 07

It is recommended that the RSST-CH results reported be viewed with caution and only as a relative means of comparing the composite and lightweight aggregate specimens. The large number of RSST-CH repetitions to only 1 percent permanent shear strain also indicates that both layers possess substantial resistance to permanent deformation at 40 °C. At higher temperatures, the results may be significantly different. The testing temperature probably should have been higher to capture the critical summer temperature in Jacksboro, Texas. This temperature may be closer to 50 °C. Further analysis of climatic data would provide a better estimate of the true critical temperature.

Assessing the predictive ability of the RSST-CH test in terms of equivalent single axle loads (ESALs) to facilitate comparison with actual repetitions of either the TxMLS or the MMLS3 proved to be difficult. First, it is suspected that the laboratory testing was not conducted at the critical temperature for permanent deformation in Jacksboro. Testing at this critical temperature is crucial in making possible conversion of RSST-CH repetitions to ESALs. The lack of control of temperature during trafficking by both the TxMLS and the MMLS3 further complicates the problem. A temperature conversion factor can be used to address this problem of temperature fluctuation for an entire year, but only a portion of the year needs to be considered in a comparison of TxMLS results and predictions from the RSST-CH. With this problem aside and assuming traffic was applied over the entire annual temperature regime, the temperature conversion factor can be used to estimate ESALs at the critical temperature in a comparison with RSST-CH repetitions at the critical temperature. Furthermore, the shift factor of 0.04 associated with converting ESALs at the critical temperature to RSST-CH repetitions is applicable only to traffic traveling at speeds faster than those associated with the TxMLS or MMLS3. The shift factor for accelerated pavement testing (APT) devices is not known at this time. Putting all of these problems aside and using the temperature conversion and shift factors as if they were appropriate, the predicted rut depth from the RSST-CH test for one of the composite specimens tested at 40 °C is smaller than the measured rut depth under the TxMLS at 100,000 axle repetitions by a factor of 8. The air voids for the Jacksboro specimens were high (approximately 9 percent), which may have had an effect on the results. The inclusion of the factor of air voids different from the 3 percent in the

analysis of RSST-CH results is still unclear at this time. The temperature for testing also has a large impact, and testing at a temperature less than the critical temperature produced the expected result of smaller rut depths. In general, the RSST-CH results cannot be related to the rut depths measured in the field.

7. CONCLUSIONS

The objectives of the Jacksboro MMLS tests were to evaluate the stripping phenomenon evident in the LWAC of the pavements in the region and to compare the relative performance of the pavement under TxMLS and MMLS3 loading. It has been demonstrated that the MMLS3 was able to distinguish, on a qualitative basis, the fatigue and rutting performance of an in-service field pavement.

In total, 1.45 million wet MMLS axles were applied to the pavement, resulting in a 62 percent reduction in the Young's modulus (SASW). Micro-cracks in the wheelpath on the surface of the pavement were also identified, suggesting that the surface layer underwent degradation resulting from the effect of water, the extent and nature of which must still be identified.

A total of 1 million dry axles was applied to the pavement with the MMLS3. A maximum rut of 1.8 mm was measured for the dry test. Preliminary indications are that the full-scale rutting under TxMLS loading is on the order of 3 times that under MMLS3 loading. Initially, this finding was the case in Jacksboro; however, a difference in the rutting mechanisms under the TxMLS and MMLS3 complicated the comparison. A limited investigation of the stress distribution beneath the TxMLS and MMLS3 loads using ELSYM5 yielded a close comparison of the permanent deformation. In view of this finding, further use of the MMLS3 as a supplemental tool to the full-scale TxMLS is warranted, despite the limitations imposed by stiff pavement surfacing layers.

As far as the proofing of the MMLS3 is concerned, the mean combined operational productivity of the MMLS3 for the wet and dry tests was 79 percent, 13 percent, and 8 percent for run, maintenance, and data collection time, respectively. This performance was considered better than acceptable.

A limited laboratory testing program was completed to further explore the distress observed under the MMLS3 trafficking. From the results of these tests, further evidence was found that the upper layers are susceptible to stripping. High shear stiffness values and RSST-CH results indicate that the upper layers of the pavement are relatively resistant to permanent deformation. The small rut depths measured under the MMLS3 correlate with these findings.

8. RECOMMENDATIONS

The degradation of the pavement under the wet MMLS3 test leads to a recommendation for similar testing on the southbound carriageway of US 281. The pavement on the southbound carriageway did not exhibit a significant reduction in Young's modulus with trafficking, which could be because the test had been conducted primarily with the pavement in a dry condition. The impact of water was yet to be determined.

To investigate the difference in rutting performance between the TxMLS and MMLS3, it is also recommended that additional MMLS3 tests be performed in Jacksboro. These tests should be performed directly on the lightweight aggregate layer by milling off

the upper 25 mm of the asphalt concrete surfacing. Such conditions will result in a higher stress level deeper within the asphalt concrete layer.

Further laboratory testing using strength and fatigue tests may provide insight into the extent and nature of distress in terms of damage caused by micro-cracking. This type of analysis is recommended to ascertain the extent of the distress manifested as a result of the moisture-sensitive surface layers.

REFERENCES

1. F. Hugo, K. Fults, D.-H. Chen, A. dF. Smit, and J. Bilyeu, "An Overview of the TxMLS Program and Lessons Learned," CD-ROM, *Proceedings of the International Conference on Accelerated Pavement Testing*, Reno, Nevada, October 18–20, 1999.
2. M. vd Ven, A. dF Smit, K. Jenkins, and F. Hugo, "Scaled Down APT Considerations for Viscoelastic Materials," *Journal of the Association of Asphalt Paving Technologists*, Vol. 67, 1998.
3. J. J. Allen, A. dF Smit, and P. Warren, "Recommendations for Establishing the Texas Roadway Research Implementation Center," Research Report 1812-S, Center for Transportation Research, The University of Texas at Austin, July 1998.
4. G. Ahlborn, *ELSYM5: Computer Program for Determining Stresses and Deformations in Five Layer Elastic System*, University of California, Berkeley.
5. M. de Beer, C. Fisher, and F. J. Jooste, "Determination of Pneumatic Tyre/Pavement Interface Contact Pressures under Moving Loads and Some Effects on Pavements with Thin Asphalt Surfacing Layers," *Proceedings: Eighth International Conference on Asphalt Pavements*, Seattle, Washington, 1997.
6. F. Hugo, D.-H. Chen, J. Bilyeu, and A. dF Smit, "Comparison of the Effectiveness of Two Pavement Rehabilitation Strategies," Draft Report 1814-1, Center for Transportation Research, The University of Texas at Austin, December 1999.
7. AASHTO T283, *Standard Method of Test for Resistance of Compacted Bituminous Mixture to Moisture Induced Damage*, Standard Specifications for Transportation Materials and Methods of Sampling and Testing, American Association of State Highway and Transportation Officials (AASHTO), 19th Edition, Part II Tests, 1998.
8. Texas Department of Transportation, *Test Method Tex-531-C: Prediction of Moisture-Induced Damage to Bituminous Paving Materials Using Molded Specimens*, Texas Department of Transportation, Materials and Tests Division, Manual of Testing Procedures, Revised August 1997.
9. R. B. McGennis, R. M. Anderson, T. W. Kennedy, and M. Solaimanian, *Background of Superpave Asphalt Mixture Design and Analysis*, National Asphalt Training Center Demonstration Project 101, Federal Highway Administration, FHWA-SA-95-003, 1994.
10. Walubita, Lubinda F., Fred Hugo, and Amy Epps, "Performance of Rehabilitated Lightweight AC Pavements under Wet and Heated Model MLS Trafficking: A Comparative Study with the TxMLS, Report 1814-3, Center for Transportation Research, The University of Texas at Austin, March 2000.

Appendix A

INITIAL DIAGNOSTIC INTERPRETATION OF THE PERFORMANCE OF MLS TEST PAD S1 IN JACKSBORO

by
FRED HUGO and ANDRÉ DE F SMIT

Nov. 1997

The performance of test pad S1 on US 281 in Jacksboro was reviewed after completion of 1.35 million MLS axle loads. To assist with the interpretation of the data that had been collected up to that point, a number of additional short diagnostic studies were performed. These studies included:

- Coring the inside and outside lanes of the southbound carriageway south of test pad S1.
- Conducting seismic tests on the pavement layers of the southbound carriageway.
- Conducting indirect tensile fatigue tests on specimens from selected asphalt cores.
- Coring in test pad S1 and conducting indirect tensile fatigue tests on prepared specimens.
- Conducting limited supplementary laboratory tests for material characterization.
- Impregnating selected cores with fluorescent epoxy to trace cracks.

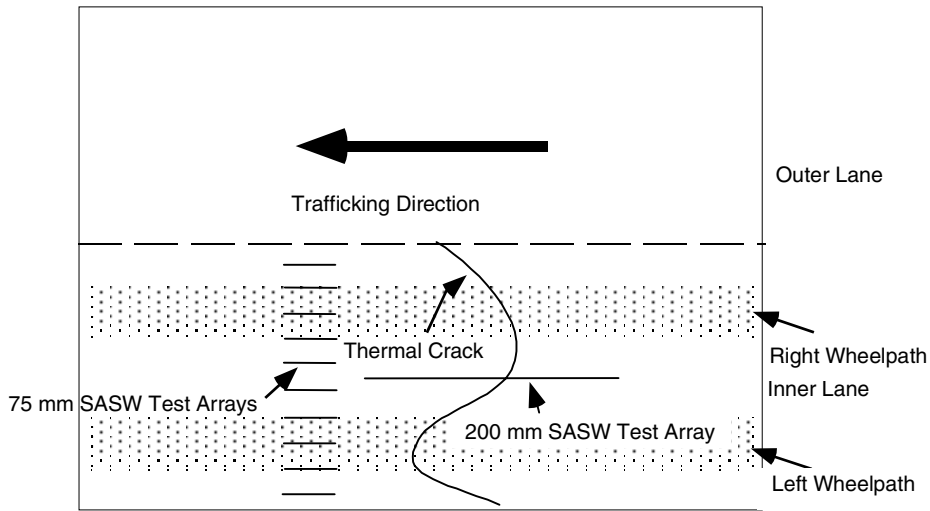
These studies were briefly reported in Tech Memo No.7, dated Nov. 13,1997, with some comment on the implications. An extract is presented below with some additional notes to serve as background to the current MMLS3 study.

1. Coring the inside and outside lanes of the southbound carriageway

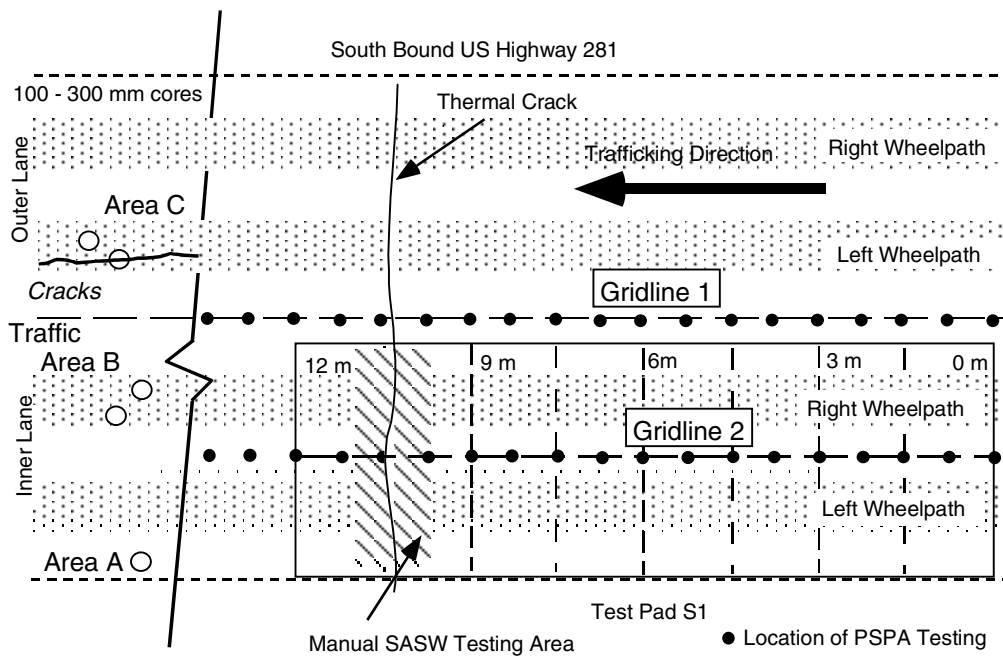
Dry coring was performed to prevent ingress of water. This exercise was very successful. The key was the use of dry ice inside and outside the core barrel to cool it. A variety of asphalt samples were taken, varying in diameter from 100 mm to 300 mm. The 100 mm diameter cores were taken to investigate fatigue resistance of the asphalt. They were taken in three areas south of the MLS test section on the southbound carriageway of US 281. Positions A and B are in the inner lane's untrafficked edge and within the wheelpath, respectively. Position C is in the outer more heavily trafficked lane's left wheelpath. These positions are shown in Figure 1.

The majority of the 100 mm specimens were from the surfacing layer of the pavement. In addition, two full-depth cores were extracted from area C, one of which was 100 mm and the other 300 mm in diameter. In these, the asphalt in the middle layer of the cores between 50 and 100 mm in depth was found to be stripped of binder. It was also moist and distressed: it disintegrated as the two cored were removed. The asphalt below this was intact, and the cores were extracted. Three test specimens having a thickness of nominally 44 mm were sawn from the full-depth cores for fatigue testing using the indirect tensile test (ITT) mode. The top cores contained the *Remixer*-processed LWAC with some fresh

aggregate added. The next cores contained the in situ LWAC (post-1986) and some old AC (pre-1986). The third and bottom cores were old AC material.



(a) Details of SASW Testing Locations



(b) Plan View of Southbound Test Site

Figure 1. Test locations for PSPA and SASW on southbound US 281 near Jacksboro, TX

2. Conducting seismic tests on the pavement layers

Seismic tests were undertaken to investigate the integrity of the asphalt mixes. The spectral analysis of surface waves (SASW) technique was used and tests were performed

at positions shown in Figure 1. The portable seismic pavement analyzer (PSPA) was also used, but the results are not discussed in this brief overview. The dispersion curves registered during SASW testing of Test Pad S1 were used to estimate the moduli of the two upper asphalt pavement layers. The results are presented in Table 1. The values are influenced by microfracturing. They are useful for comparing relative performance between test sections and changes that occur during trafficking.

Table 1. Moduli determined from SASW dispersion curves test pad S1 after trafficking (MPa)

Layer	Trafficking				
	0	40k	300k	750k	1.2m
0-50 mm	3337	6289	4000	2300	2100
50-110 mm	1201	1830	1073	970	868

To gain insight into the rate of deterioration of the asphalt under the conventional traffic, the Young's Modulus of the two top layers of asphalt was measured by means of Crosshole testing (Woods and Stokoe, 1972). Tests were conducted on samples cored from areas A, B, and C (see Figure 1). The top 50 mm is the *Remixer* recycled lightweight aggregate asphalt (LWAC), and the next nominal 50 mm is the original lightweight aggregate asphalt. This layer's thickness varied along the test section and was generally approximately 25 mm thick. The results of the crosshole tests are shown in Table 2. The effect of trafficking on modulus is apparent. The moduli all reduced with increased traffic, but the rate of reduction was greater in the lower layer. Currently the modulus of the outer wheel path is only 21% of the virgin modulus in the untrafficked edge area of the inner lane.

Similar trends were measured when the SASW tests were performed prior to the start of the MLS testing. This can clearly be seen in Figure 2, which depicts the composite modulus values measured across the width of the lane at the position shown in Figure 1.

3. Conducting ITS fatigue tests on selected asphalt cores from the southbound carriageway

Stress-controlled repeated load fatigue tests in the ITT mode were done on the specimens obtained from coring using a closed-loop electrohydraulic Materials Testing System (MTS). A haversine load function with a preload of 100 N and a nominal load amplitude of 2,000 N was used for a specimen width of 44 mm. The testing frequency was 10 Hz, and the test temperature was 20 °C. The test specimens were all set up with the load along the line of traffic. During the fatigue testing and after 100 loading cycles, the vertical deformation of the loaded specimens was measured.

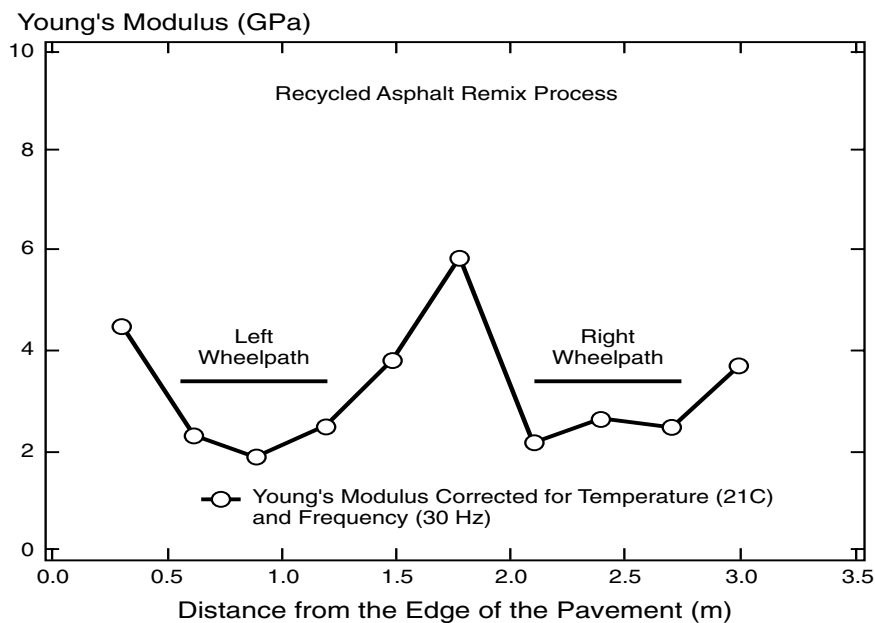
Table 2. Results of crosshole testing of the top two asphalt layers at three locations on US 281, Jacksboro, TX

(a) Top 50 mm Remix Recycled Asphalt				
Locations	Location in Fig. 1*	Young's Modulus **MPa	% of Virgin Shoulder	Condition of Cores
Shoulder	A	3036	100%	Intact
Wheelpath on Inner Lane	B	2807	92%	Intact
Wheelpath on Outer Lane	C	2073	68%	Intact

(b) Original Lightweight Aggregate Asphalt Layer Between depths of 50 and 100 mm				
Locations	Location in Fig. 1*	Young's Modulus **MPa	% of Virgin Untrafficked Edge Area	Condition of Cores
Shoulder	A	2404	100%	Intact
Wheelpath on Inner Lane	B	1676	70%	Intact
Wheelpath on Outer Lane	C	509	21%	Microfractured and Stripped

* Note : Locations of test areas are shown in Fig. 1.

** From Crosshole test at mid depth of the respective layers.



Jacksboro, TX, using SASW

Figure 2. Young's modulus measured across the pavement in southbound US 281

This value was selected to represent about 30% of the indirect tensile strength of the asphalt mixes. The number of cycles until complete failure of the specimens was recorded. The permanent deformation of the specimens during the fatigue tests was also monitored. Table 3 below shows the mean values of the material properties as measured during the fatigue tests. The important finding was that the fatigue life of the trafficked cores was only 10% of that of the untrafficked cores. It was interesting to find such a long fatigue life for the specimen from the bottom of the asphalt layers (see comments later). It was apparent that the surface had undergone severe distress. This was in accordance with the SASW test results that showed a loss of stiffness.

Table 3. Repeated load fatigue test results

	Trafficked Top Layer	Trafficked Bottom Layer	Untrafficked Top Layer
Number of Specimens	4	1	4
Stiffness (MPa)	2 592	2 538	2 614
Fatigue Life N_f (cycles)	10 020	150 000	106 700
Deformation Rate (mm/million cycles)	285.8	8.4	16.3

The deformation rates shown in Table 3 were measured for the constant rate of deformation before specimen failure. These rates do not necessarily reflect rutting resistance of the different layers, as the crack growth during fatigue must be taken into account. It should be noted that the fractured surfaces of the trafficked cores in the outer lane all exhibited signs of stripping. This was not observed in the cores from the inner lane.

4. Coring in the test pad S1 for testing relative fatigue strengths and other material characteristics

After testing the outside cores from the conventionally trafficked pavement south of test pad s1, cores were taken from test pad s1 to explore the condition of the pavement after TxMLS trafficking. Figure 3 shows the positions where cores were taken. The results of the findings are shown in Tables 4a, 4b and 4c, for the top, middle, and bottom layers. It must be stressed that the tests were done at a fixed stress level regardless of the mixture type or composition. This meant that it could be expected that the results of the different layers would vary and not be comparable, except with respect to cores taken from the same layer.

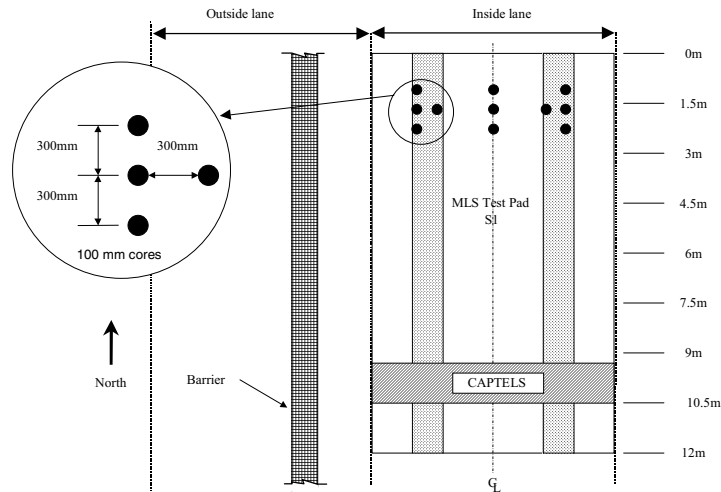


Figure 3. Locations of cores taken for testing condition of the asphalt layers in test pad S1

From the results it was again clear that the middle layer was the weakest, and furthermore the right wheel path showed a marked difference in the degree of distress compared to the left wheel path. The top layer specimens had a longer fatigue life than those from the outside surface layers, indicating that they had not deteriorated as much under the MLS as the layers under conventional traffic. It must of course be remembered that performance is dependent upon the entire structure and a more in-depth study was necessary before final conclusions could be drawn.

The stiffnesses of the trafficked and untrafficked cores did not differ significantly and it is thought that this could be because measurements are made in compression in the indirect tension mode. This mode would be insensitive to changes in the tensile stiffness of the samples.

Table 4a. Repeated load fatigue test results, top layer — Test pad S1

	Trafficked Top Layer	Trafficked Bottom Layer	Untrafficked Top Layer
	Left Wheel Path	Right Wheel Path	Between Wheels
Number of Specimens	2	2	2
Stiffness (MPa)	2 740	2 717	2 568
Fatigue Life N_f (cycles)	57 580	35 450	48 250

Table 4b. Repeated load fatigue test results, middle layer — Test pad S1

	Trafficked Top Layer	Trafficked Bottom Layer	Untrafficked Top Layer
	Left Wheel Path	Right Wheel Path	Between Wheels
Number of Specimens	2	2	2
Stiffness (MPa)	2 633	2 650	2 506
Fatigue Life N_f (cycles)	41 902	1660	12 350

Table 4c. Repeated load fatigue test results, bottom layer — Test pad S1

	Trafficked Top Layer	Trafficked Bottom Layer	Untrafficked Top Layer
	Left Wheel Path	Right Wheel Path	Between Wheels
Number of Specimens	2	2	2
Stiffness (MPa)	2 953	2 670	2 683
Fatigue Life N_f (cycles)	221 662	4 775	184 650

4.1 Characterizing Materials

To gain insight on the performance of the asphaltic materials, gradation analyses were done dry on samples (2000 g) from the upper 50 mm of cores from trafficked and untrafficked sections. Figure 4 shows the gradation of the aggregates (extracted using the vacuum extraction method) from the trafficked and untrafficked cores plotted on a 0.45 power chart with SUPERPAVE™ control points and restricted zone. This was to capture aspects of validation of the system should they manifest during the implementation phase.

The aggregate was lightweight and extremely porous. This type of aggregate has been known to crush under construction and heavy traffic. The gradation curves as shown are therefore not necessarily indicative of the design gradations. The gradation of the trafficked aggregate is coarser than the untrafficked. This is contrary to what one would expect and without a detailed study of the constructed layers, it is not possible to say why this was so. Both gradations pass through the restricted zone, the trafficked on the lower side, the untrafficked on the upper side. Both gradations fall within the SUPERPAVE™ control points. The gradations appear to run parallel to the maximum density line.

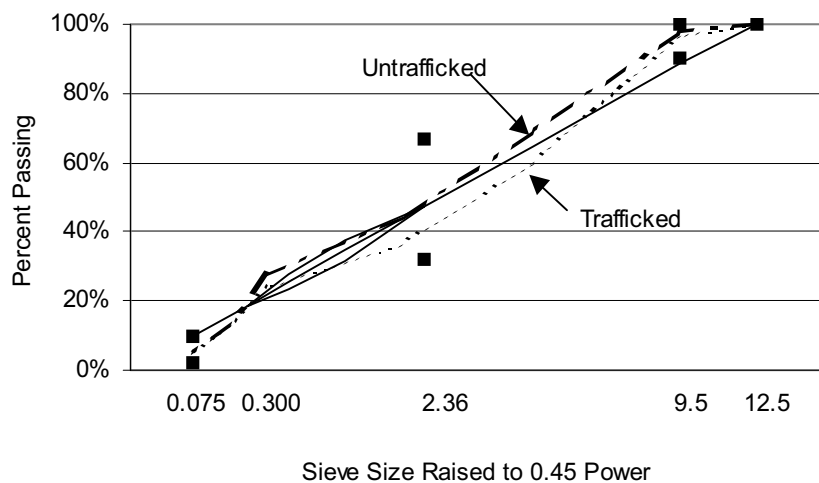


Figure 4. Aggregate gradation curves

4.2 Bitumen Properties

Binder was extracted and recovered from the trafficked and untrafficked cores taken outside the test pad using the Abson method according to the TxDOT Manual of Testing (Texas Department of Transportation, 1996).

Table 5 shows the results of standard penetration and softening point tests. The results indicate hardening of the bitumen with traffic.

Table 5. Standard bitumen test results

	Trafficked	Untrafficked
Penetration @ 25°C 0.1mm	23	29
Softening Point °C	58	55
Penetration Index	-1.01	-1.19

Dynamic shear rheometer (DSR) tests were also conducted on the extracted bitumen. The tests were performed at three different temperatures. The dynamic shear complex moduli (G^*) and phase angles (δ) of the bitumen from the trafficked and untrafficked cores are shown in Figure 5 and Figure 6, respectively. Once again the bitumen from the trafficked cores appears stiffer.

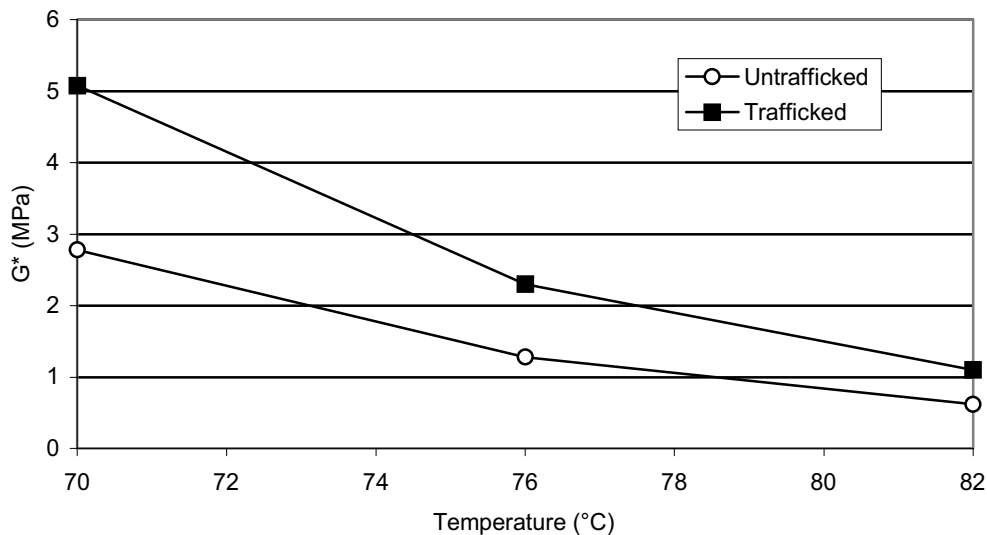


Figure 5. Dynamic shear moduli of extracted bitumens (DSR)

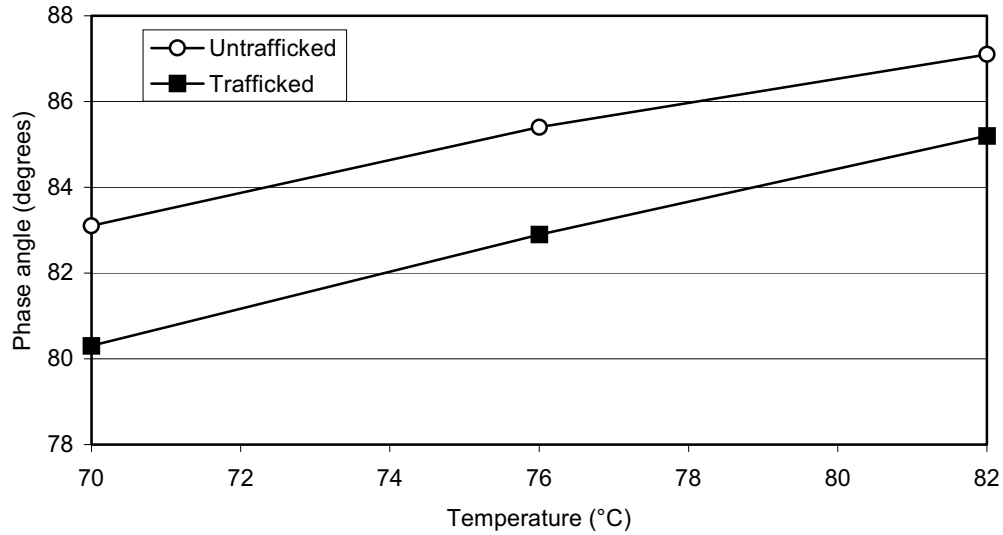


Figure 6. DSR phase angles of extracted bitumens

4.3 Shear Frequency Sweep Testing (FSCH)

Shear frequency sweep tests were done on the top and bottom sections of the 150 mm diameter cores taken from the untrafficked areas outside the TxMLS S1 test pad. The tests were done at ten different frequencies and three different temperatures. Figure 7 shows the master curves for shear stiffness for different frequencies and Figure 8 shows the corresponding phase angles. From these figures it can be seen that the stiffness of the top layer is slightly greater than the bottom layer. However it should be remembered that the bottom layer is a composite containing some of the layer below it. At higher temperatures the stiffness is sensitive to test frequency, although this sensitivity decreases at the higher test frequencies.

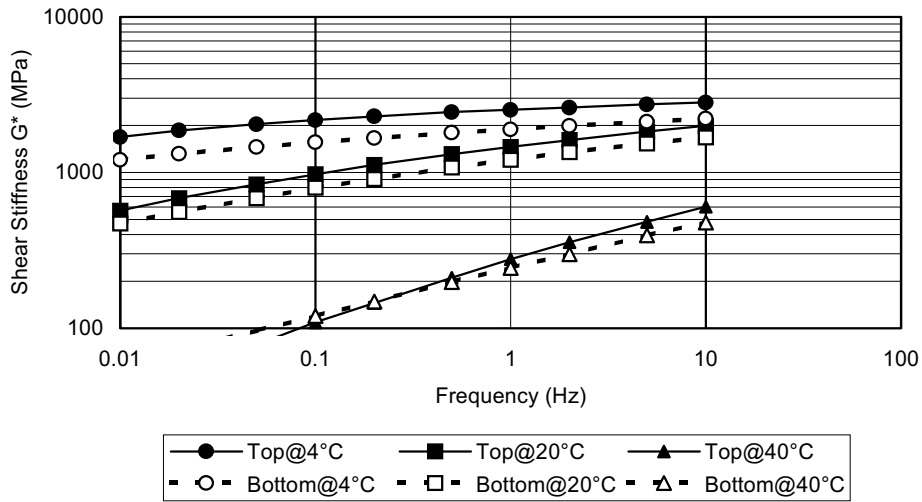


Figure 7. Master curves for shear stiffness (untrafficked cores southbound US281)

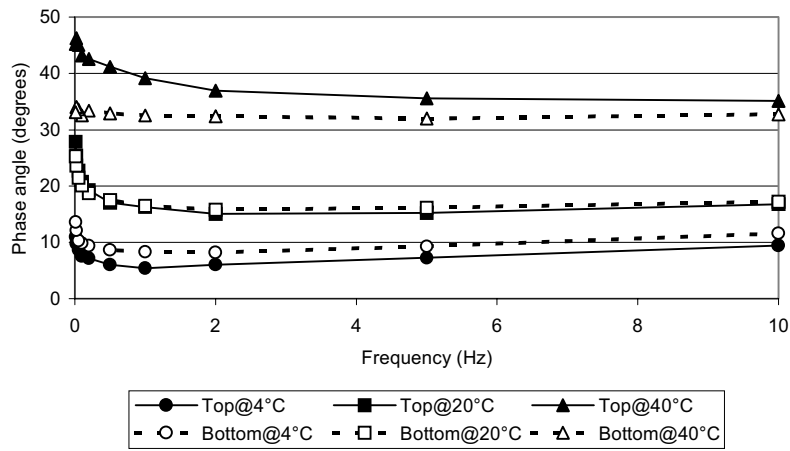


Figure 8. Phase angle response of shear frequency test samples (untrafficked cores southbound US 281)

4.4 Simple Shear Tests at Constant Height (SSCH)

Simple shear tests at constant height (SSCH) were also performed on the top and bottom sections of 150 mm diameter cores taken from the untrafficked areas outside the TxMLS S1 test pad. These tests were conducted at three different temperatures (4, 20, and 40 °C) to examine the physical response of the mix. Figure 9 shows the load functions that were applied at the different temperatures, and Figure 10 shows the shear deformation response of the specimens under loading. The results indicate that there is not a significant difference in the permanent strain under loading between the upper and lower layers at low to moderate temperatures, although at 40 °C, the lower layer appears to be more susceptible to permanent deformation.

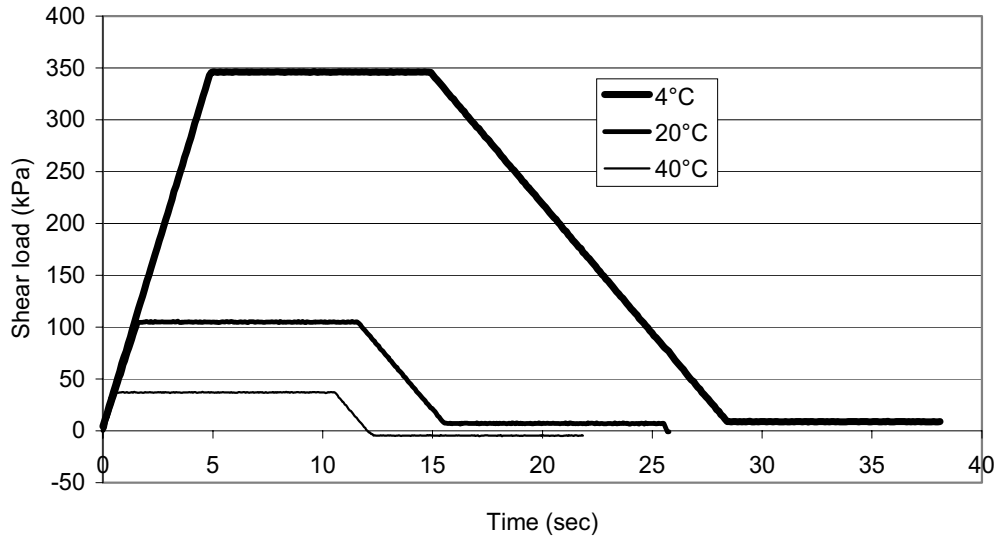


Figure 9. Load vs. time during shear testing at different temperatures

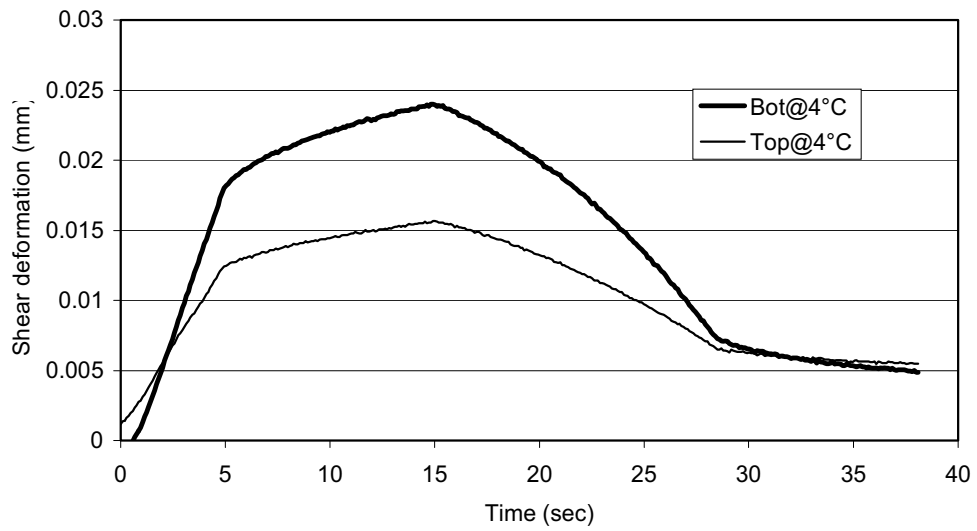


Figure 10 (A) 4 °C

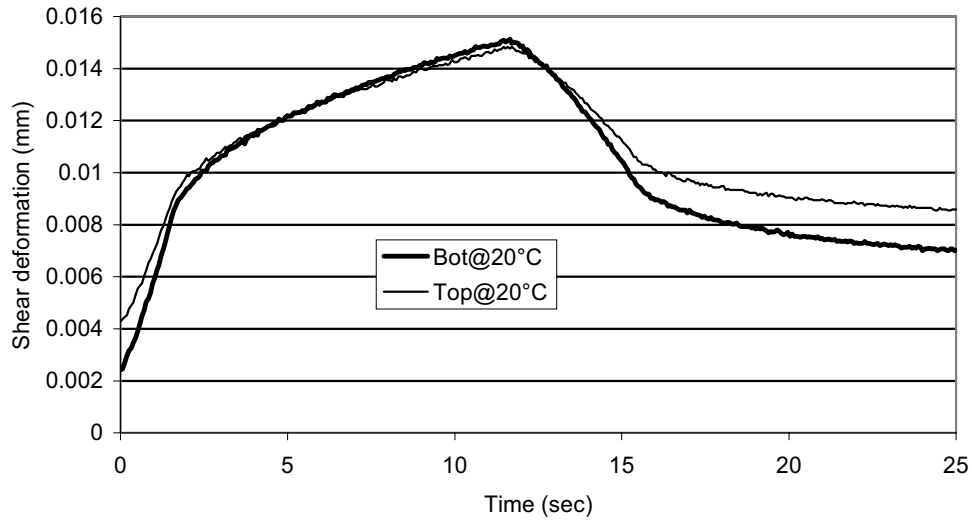


Figure 10 (B) 40 °C

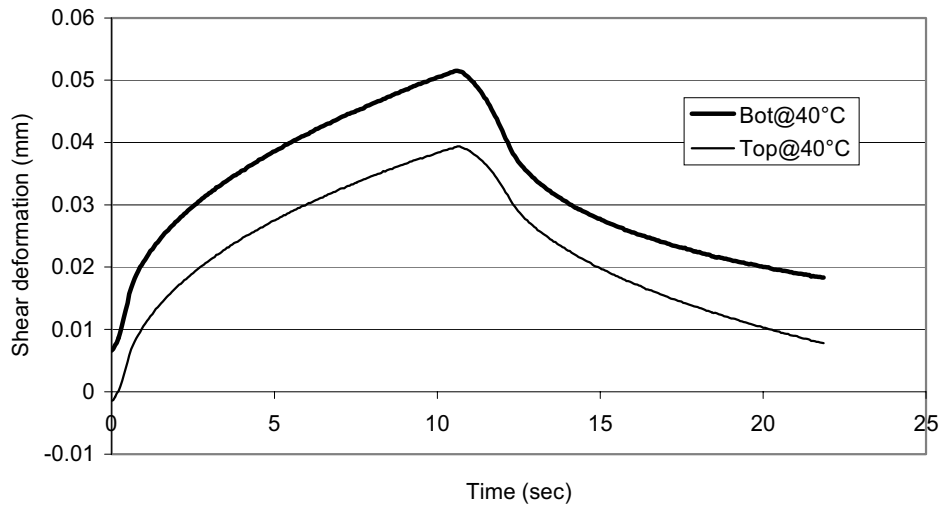


Figure 10 (C) 40 °C

Figure 10. Deformation vs. time during shear testing at different temperatures

4.5 Volumetric Properties

Table 6 shows the calculated volumetric properties of the trafficked and untrafficked cores. Maximum theoretical relative density was determined as 2.237. The bulk density of the aggregate was unknown, and for this reason binder absorption was estimated at 2%.

Table 6. Volumetric properties of trafficked and untrafficked cores

	Trafficked		Untrafficked	
	Mean	StDev	Mean	StDev
Number of Specimens	6	-	4	-
Bulk Relative Density	2.115	0.016	1.927	0.019
Voids in mix	5.4%	0.7%	13.9%	0.8%
Binder Content	8.1%	-	7.1%	-
Voids in Mineral Aggregate	18.5%	0.6%	23.8%	0.7%
Voids Filled with Binder	70.6%	3.0%	41.8%	1.7%
Filler Content	4.6%	-	5.0%	-
Dust Proportion	0.75	-	0.98	-

5. Impregnation of Selected Cores with Fluorescent Epoxy

To determine the extent of microfracturing and fatigue under trafficking, selected cores were impregnated with fluorescent epoxy and then cut along the line of traffic. The cut surfaces were then inspected under UV light. The following was observed:

- There were indications of surface cracking in the upper layer (Figure 11):
- The lightweight aggregate asphalt from the outer lane had intrusion throughout the layer (Figure 12).
- The core from the bottom of the asphalt layers had very little intrusion and was apparently very dense (Figure 13)

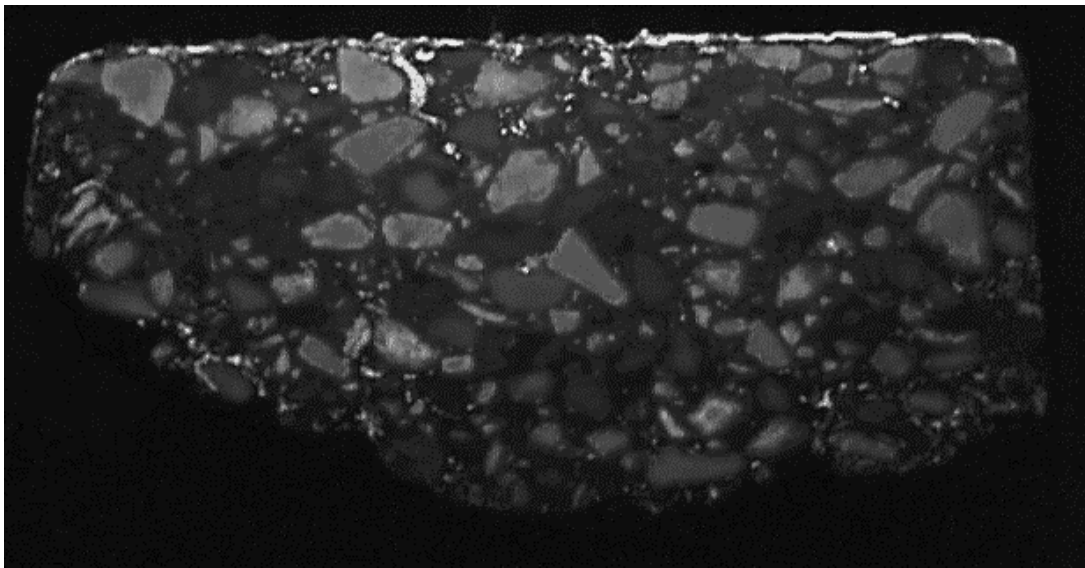


Figure 11. Epoxy-impregnated upper layer

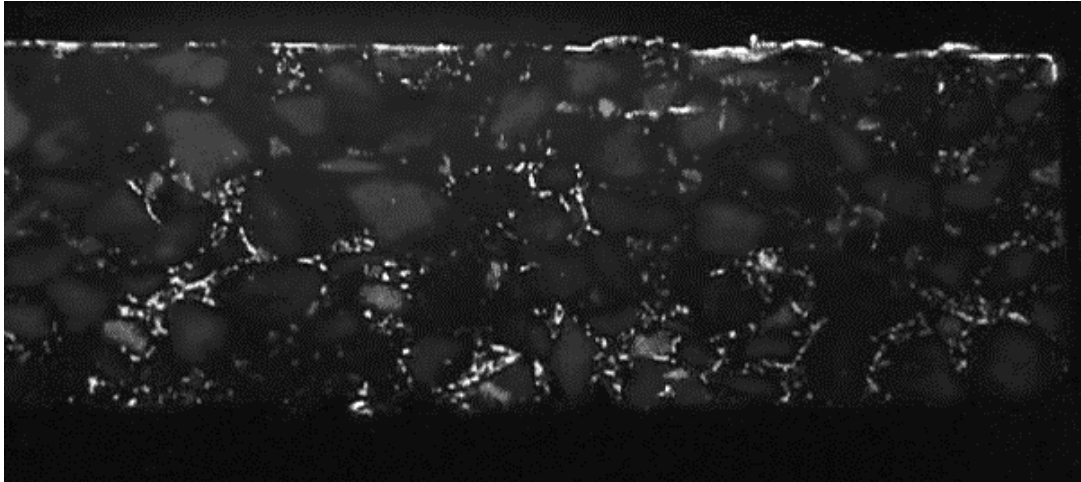


Figure 12. Epoxy-impregnated middle layer

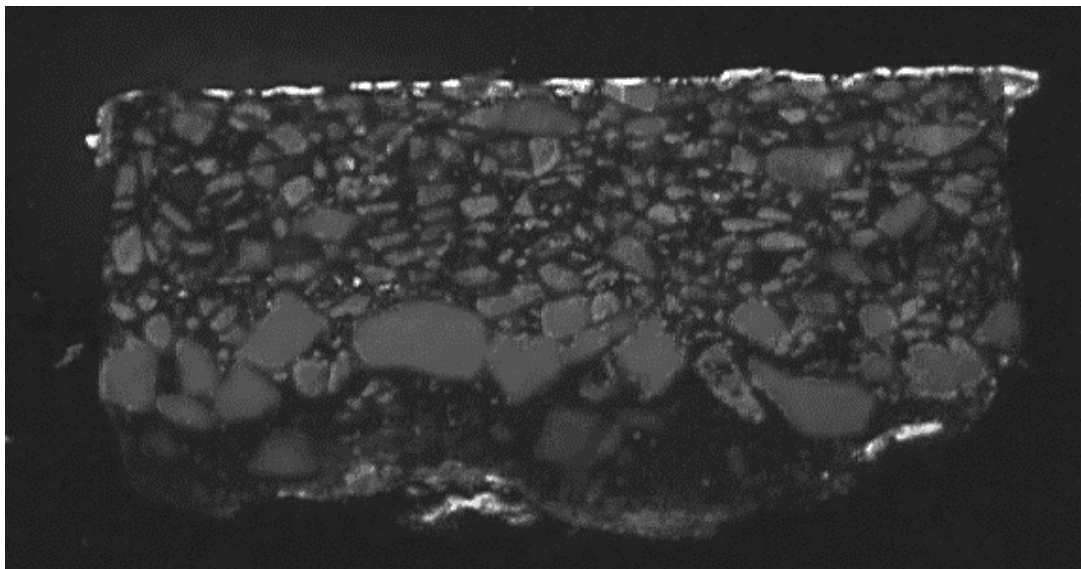


Figure 13. Epoxy-impregnated bottom layer

Synthesis of the Findings

The important finding has been the reduction in modulus, which appears to be related to distress in the upper asphalt concrete layers. It was apparent that the reduced modulus occurred as a result of microfracturing of the underlying lightweight aggregate asphalt and subsequent stripping of the binder. This was probably due to the shear in the layer and the influence of trapped moisture under the densified new recycled material.

During the MLS trafficking, SASW measurements were performed intermittently. The composite modulus values of the total asphalt layer are shown in Figure 14.

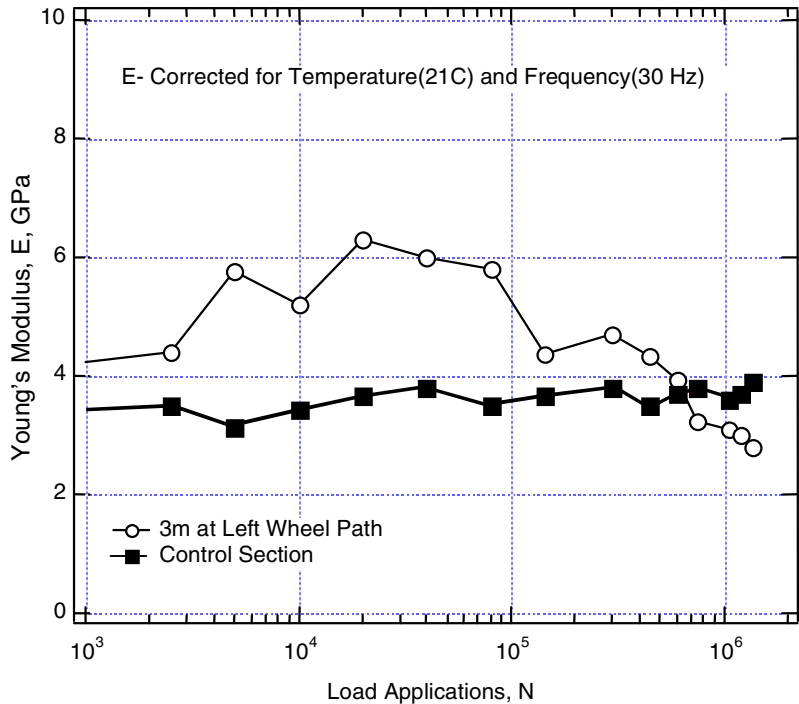


Figure 14. Corrected Young's modulus vs. number of axle loads (up to 1.35 million) using SASW US 281, Jacksboro, TX

It can be seen that the untrafficked control area remained approximately constant at 3.5 G Pa. By contrast, the trafficked area showed a marked increase from the initial 4 G Pa to 6.5 G Pa at 20,000 axle load repetitions. Then it slowly dropped to just below 6 G Pa at 80,000 repetitions, whereafter it rapidly fell to nominally 2.65 G Pa after 1,350,000 axles.

The increase in modulus is considered to be owing to the consolidation of the recycled asphalt under trafficking. The initial voids of the untrafficked surface layer were 12% to 13%. The subsequent sharp drop in modulus is thought to be due to microfracturing of the lightweight aggregate asphalt and subsequent stripping of the binder. No visible cracking has yet been observed on the surface, but there are signs of flushing — probably a result of the binder flowing up from the underlying stripped layer.

In the trafficked wheelpath of the outside lane it was found by coring that the voids had reduced by 7–8%, probably owing to a process similar to that outlined above.

The results of the fatigue tests indicate that the surfacing layer of the conventionally trafficked section is already in an advanced stage of distress. Initial indications are that the distress is in the form of surface cracking. This assessment was not investigated further.

The fatigue specimens were retained for additional testing. A test program that included the determination of the maximum theoretical density, the bitumen content, and gradations of

the trafficked and untrafficked specimens was undertaken. The binder was extracted and tested.

From the data that have been collected thus far, and from the information presented above, the following scenario appears to be the most probable:

1. The recycled asphalt concrete surfacing had high “after-construction” voids. This situation permitted moisture to enter the layers. However, upon trafficking, the voids progressively closed. This action happens much faster under APT than under conventional traffic.
2. As the voids reduce, the layer becomes less permeable in the wheel path. Water is still able to enter outside the wheel path. This situation can lead to “damming” of the water as it flows downhill.
3. Under trafficking, pore pressure develops in the underlying lightweight aggregate asphalt layer. This pressure development reduces its modulus and shear strength and ultimately leads to stripping and eventually failure of the pavement layer. The rate at which this occurs is dependent upon the rate of trafficking and the environmental conditions prevailing during trafficking. It should be noted that the effect of regular automobile tires on stripping would also have to be considered in terms of trafficking, since stripping is dependent on the mechanism of failure.

On the assumption of the foregoing hypothesis, the pavement should exhibit performance characteristics associated with the events. This means that the shoulder of the inside lane should be least affected and the outside lane’s wheel path should be in the worst condition. In the same vein, the second layer of the pavement should be experiencing faster deterioration than the surfacing layer. This is exactly in accordance with the findings presented above.

The implications of the above scenario on the APT section need to be considered. It is uncertain what the condition of the pavement of test section S1 is, but it appears that its condition is better than that of the outside lane, which had only conventional traffic on it for less than 3 years.

Relevance of the Findings

It is apparent that the testing in Jacksboro has thus far yielded a number of significant findings that have a direct impact on the entire MLS program. These findings are indeed highly relevant to APT programs as a whole. In summary, the following aspects require consideration:

- The SASW testing was able to detect changes in the modulus of the asphalt under trafficking and related distress as a result of the presence of moisture. Ground penetrating radar (GPR), which is also being used in the test program as a means of improving quantification of appropriate benchmarks of performance, is yielding performance indicators similar to those yielded by the SASW.

- With the testing of the rehabilitation test pad in Jacksboro, the change in modulus as trafficking progressed could be explained by a difference between the volumetric structure of the recycled asphalt and the underlying old asphalt. As the new asphalt was being trafficked, it was probably being further compacted and bonded more intimately to the lower layer. A reduction in air voids was also found in the Victoria TxMLS tests. At the same time, the shear stresses in the lightweight aggregate asphalt were probably causing microfracturing, leading to the ingress of water and stripping. Such action would cause the binder to be pumped upwards into the high voids of the top layer, blocking the escape route for trapped moisture. Such action would also explain the drop in the modulus of the second layer.
- From an analysis of the rainfall records in the Jacksboro area it would appear that the S1 test section has had about the equivalent of 3 years or less of rainfall during trafficking. The basis for the analysis was the number of axle loads during rain with due regard to the fact that the test section is also covered by the TxMLS. This fact should explain the difference in performance between the outer lane and the test section.
- The relationship among SASW modulus, traffic, and related distress has now been sufficiently well established to warrant its use as a pavement management tool. This idea should be considered an important outcome of the TxMLS program. As an interim guide, it is suggested that a drop to 70% of the original value of the modulus be taken as a signal to perform a diagnostic investigation. A drop to 50% could mean irreversible damage.

Conclusions

There is clearly an urgent need to gain greater insight into the current condition of the two upper pavement layers of test pad S1 and to test the validity of the hypotheses on moisture damage presented in the Tech Memo, otherwise the MLS program could be jeopardized.

The best and probably only way of achieving this would be to take cores from test pad S1 according to the test protocol submitted on September 22, 1997. Furthermore, it would seem advisable to subject the pavement to some form of water ingress during trafficking to bring the performance of the pavement closer to the condition of the existing outer lane.

Acknowledgements

James Lee (CTR) and Sydney Greer (TTI) assisted the authors with the laboratory and field studies that formed the basis of this diagnostic evaluation. TxDOT staff assisted with field sampling. The Superpave Center was responsible for the Superpave testing of the binders and cores.

References

Woods, R. D., and Stokoe, K. H., II (1972). "In-Situ Shear Wave Velocity by Cross-Hole Method," *Journal of the Soil Mechanics and Foundation Division*, Proceedings, ASCE, Vol. 98, No. SM5, May 1972, pp. 443-460.

Texas Department of Transportation (1996). *Recovery of Asphalt from Bituminous Mixtures by the Abson Process*, Manual of Testing Procedures, Volume 1, Tex 211-F.

APPENDIX B. NOTES ON OPERATING THE MMLS3 PROTOTYPE

- 1 Remove the machine from its transport packaging. The machine is strapped to a wooden pallet, the combination of which can be handled by either a forklift or a crane. The crane should be attached to the single shackle on top of the machine. Once removed from the pallet, the machine should not be handled by a forklift, which will damage its underside. Once off the pallet, the machine can be moved around on its own transport wheels or lifted by crane.
- 1.1 Remove the two nylon straps and the 10 mm iron rod that ties the two vertical wooden beams together. The rod can be removed by removing the two outside nuts and pulling the two beams away from each other to disengage the rod from the holes in the beams, one side at a time.
- 1.2 Using a crane, lift the machine from the pallet by the single shackle on top. **DO NOT SET THE MACHINE DOWN.**
- 1.3 Take the base plates and transport wheels from the pallet.
- 1.4 If the machine is to be placed directly in position onto the test pavement, it is not necessary to attach the transport wheels. Place the base plates in position on the pavement so that the color codes (blue and yellow) will line up with the same colored marks on the machine. Carefully lower the machine so that the four rods of the adjustable feet fit into the bearings on the base plates. It may be necessary to rotate the rods to facilitate the engagement.
- 1.5 If the machine has to be moved around on its own wheels, mount the three wheels while the machine is still hanging from the crane and lower it to stand on the wheels.
- 1.6 Remove the expanded metal protection cover on top at the drum side by removing the bolts and nuts with a 10 mm spanner. Remove the four spare tires. Do not replace the cover yet.
- 2 Inspect the machine for damage.
- 2.1 Visually check for bent or broken parts.
- 2.2 With a feeler gauge, check the gap between the ends of the two upper rails and the drive drum where the rails meet the drum. It should be between 8 and 20 thousandths of an inch. If the chain of bogies has to be moved by hand, grab it only by one of the round wheel axles of the link sections between bogies to avoid injury. If the gap is not correct, try to find out what caused the movement and readjust the gap as described under 6.2 below.
- 2.3 Plug the red four-pin connector on the motor control unit into the socket on the side of the machine. Plug the control unit into a 220V AC supply. Push the JOG button. The chain of bogies should move at a constant slow speed (about 200 mm/sec). Let it run for at least one revolution to make sure that it is free to move.
- 2.4 Disconnect the control unit.
- 3 Set the wheel load. The wheel load on the pavement is set by adjusting the suspension springs on the bogie. After that the load is virtually independent of the displacement of the suspension (see 4.2 below). A calibration unit has not been supplied, but the springs have been preset for the correct load. Two sets of springs are supplied. The springs mounted in the machine have been

set to a load of 2.1 kN (for a tire pressure of 690 kPa). The spare set has been set to 1.05 kN (for a tire pressure of 345 kPa). To use the latter load the springs have to be swapped. Proceed as follows:

- 3.1 Find the two 12 mm nuts and two sleeves tied to the cable of the control unit. Push a sleeve, smallest diameter end first, over the open end of each of the two suspension spring rods on a bogie, followed by a 12 mm nut. Using a 19 mm spanner, tighten the nut on one of the springs to compress the spring about 3 mm, taking the load off the pin on the opposite side.
- 3.2 Using circlip pliers, remove the circlip from the pin and pull the pin out. Lift out the spring.
- 3.3 Replace the spring with the correct one from the other set. The springs are marked with punch marks that should correspond with the marks on the pin housing. Note that the left- and right-hand side springs for each bogie are marked differently. For the wheel load to be correct it is important to mount each spring in its correct position.
- 3.4 Remove the nut and sleeve from the mounted spring and repeat the operation on the other spring on the same bogie. It is important to remove only one spring per bogie at a time.
- 3.5 Adjust the tire pressure if necessary
- 4 Set the machine up on the pavement.
 - 4.1 Get the machine in position.
 - 4.1.1 Move the machine in positions on the test pavement on its transport wheels.
 - 4.1.2 Slide the base plates in underneath the machine from the sides so that the color markings line up with those on the machine frame.
 - 4.1.3 Adjust the rods of the feet so that they fit into the four bearings on the two base plates.
 - 4.1.4 Raise the machine to its maximum height and remove the three transport wheels. Avoid twisting the frame by allowing it to stand on two diagonal feet only. Adjust the two feet at one end of the machine simultaneously and observe the bubble in the spirit level mounted on top of the frame.
 - 4.1.5 Lower the frame evenly until the rubber wheels are between 10 and 30 mm from the ground and attach the links between the base plates and the lever arms for lateral displacement. The frame can be pushed sideways on the base plate rollers to line up the links. One side needs a 17 mm spanner and the other side a 6 mm Allen key and a 13 mm spanner. Tighten the lock nuts.
 - 4.2 Adjust the height. The load of the wheels on the pavement is determined by the spring settings and is virtually independent of displacement. (See “Set the wheel load” under No. 3 above.) The total travel of the wheel suspension is about 20 mm. It is best to set it in the center of this range and to lower the frame progressively as rutting in the pavement develops.
 - 4.2.1 Look through the large inspection opening in the side of the machine and move any one bogie until the forward four of its six yellow wheels are just out of the curve coming down on the opposite side of the drive drum, and onto the start of the bottom straight rail section. The bogies may be moved by hand or by using the JOG function of the control unit. To avoid injury when

- moving it by hand, do it only by the round axles of the yellow wheels of the link sections between bogies.
- 4.2.2 Evenly lower the machine until the two black rubber stoppers at the end of the trailing arms that holds the rubber wheel just start to move away from the metal plate underneath it.
- 4.2.3 DISCONNECT THE MOTOR CONTROL UNIT FROM THE MAINS. Find the PVC gauge, shaped like a human leg and foot, that was tied to the cable of the motor control unit. The “toe” of the gauge is 8 mm high, increasing to 10 mm where it is attached to the “leg.” Holding the gauge by the “leg,” measure the gap underneath the rubber stopper. Only one of the two stoppers needs to be checked. Lowering the machine will increase the gap and vice versa. The setting is correct when the “foot” fits in the gap with little or no clearance. A tolerance of 1 or 2 mm to either side is allowable.
- 4.2.4 Move the bogie forward until the forward two of its six yellow wheels are just at the end of the bottom straight rail section. ALWAYS DISCONNECT THE MAINS SUPPLY BEFORE WORKING INSIDE THE MACHINE. Check to ensure that the gap is still about the same. If it is not, adjust the two feet at that end of the frame to correct it, even if it means that the machine is not standing horizontal lengthwise.
- 5 Run the machine.
- 5.1 Set the machine up as described under No. 4 above and tie the adjusting handles of the two feet at each end together with a piece of string to prevent them from creeping downwards during operation.
- 5.2 Connect the motor control unit and the power supply for the lateral movement to the machine and to a 220 VAC supply. Total consumption is about 1.5 kW.
- 5.3 Always first use the JOG function on the control unit for at least one revolution of the bogie chain to make sure that the machine is clear to run.
- 5.4 When the control unit is switched on it displays output frequency in Hz. If the START button is pressed, the motor will run at the displayed frequency. To change the speed, push the RIGHT arrow until the digit to be changed flashes and use the UP or DOWN arrows to change the value; then press ENTER, which can be done with the motor stationary or running. Any change will take effect only after the ENTER button has been pressed. The maximum frequency that can be set is 55 Hz, at which speed exactly two wheels per second passes a fixed point (7,200 wheels per hour).
- 5.5 With the machine running, press DISPLAY until the motor current is displayed in amps (A). The current at full speed should stay below 4.1 A. A higher current indicates a problem somewhere. Stop the machine and investigate. The unit will trip at about 5A.
- 5.6 The lateral displacement system automatically switches on when the main motor runs at more than about 20 Hz and switches off when it is stopped or slowed down to below that speed.
- 5.7 The wheel counter works only when the main motor runs at above about 40 Hz.

- 5.8 After a few millimetres of rutting has developed, it may be necessary to stop the machine and readjust the suspension gaps as described under No. 4.2 above.
- 6 Maintenance:
- 6.1 The yellow (polyurethane) wheels: The two wheels in the centre of each bogie (in line with the axle of the rubber wheel) carries nearly all the load. Inspect them every few hours for signs of deterioration. Eight spare wheels with bearings are supplied. The wheels can also be exchanged with the other wheels on the bogie that carries less load. Please note that the wheels fitted on the link sections are made from cast iron, while those on the bogies are aluminum. Do not use different types on the same axle. The aluminum wheels have a greater load capacity. You will find that some of the small circlips retaining the wheels on their shafts are missing. This is not important, as the wheels cannot come off, even without the circlips.
- 6.2 The gap between the rails and the drum: Where the top and bottom rails meet the rotating drum that drives the bogies around, the gaps between the drum and the rail ends are about 15 thousandths of an inch. The shaft of the drum is mounted on horizontal slides and is spring loaded in the horizontal direction to pinch the yellow wheels between the drum and the outer rail. When the machine operates there are small horizontal movements of the drum that may wear the slides. This movement can cause the drum to displace vertically, changing the sizes of the gaps mentioned above. It is thus necessary to check the gaps from time to time with a feeler gauge. It is necessary to measure the gaps only on the top side, assuming that if they are correct, the bottom ones will be correct as well. The gaps should be between 0.008 in. and 0.020 in. at the narrowest position. Excessive vertical displacement of the drum will cause the drum to scrape against the rail ends either at the top or bottom. This situation will cause a scraping sound and the motor will draw more current to overcome the additional friction. Monitor the motor current as described under No. 5.5 above. The prototype machine does not have a fine adjustment mechanism to set the gaps. Should the gaps need adjustment, proceed as follows:
- 6.2.1 Release the two 13 mm nuts on the bottom slide (below the bearing on the drum shaft) on the same side of the machine where the gap needs adjustment, about half a turn.
- 6.2.2 If the gap on top of the drum needs to be increased, lightly tap the shaft or bearing downwards with a hammer. If necessary, further release the nuts. Measure the gap with a feeler gauge and set it as close to 0.015 in. as possible, but between 0.008 in. and 0.020 in. Tighten the nuts, but do not over tighten.
- 6.2.3 If the gap needs to be reduced, use a block of wood about 20 mm thick and 100 mm high and place it on the beam right underneath the slide. The top of the block should be at the same height as the bottom of the lower slide. Release the nuts and, using a large screwdriver right below one of the nuts, lever the slide upwards and tighten the nut. Repeat for the other nut until the

- gap is the correct size. It may be necessary to release the nuts on the upper slide and to allow enough upward movement of the drum.
- 6.3 After operations 6.2.2 or 6.2.3 above, release the nuts on the upper slide and push the slide down to eliminate excessive free play. Tighten the nuts. Do not overtighten.
 - 6.4 Repeat for the other side of the machine.
 - 6.5 Check to see that the slides are still free to move. Run the machine. There should be slight horizontal movements (about 0.5 mm) of the plate onto which the bearing is mounted; otherwise the slide is too tight. In such a case, release the two nuts on the upper slide slightly until movement can be observed. Retighten the nuts. Do not overtighten.

Notes on the lateral movement

- 1 The motor is 24 volt DC, 90 watt.
- 2 The power supply delivers 24V DC, full-wave rectified, but not smoothed.
- 3 The two-pole relay with the 220V coil is used to switch off the DC motor when the main (220V three-phase motor) stops. The coil of this relay is wired parallel to one of the phases of this motor. The contacts of the relay are wired in series, with the current from the power supply in a normal/open configuration.
- 4 The large limit switch is wired in series with the 220V coil of the relay to stop the lateral movement should it overrun one of the small limit switches. This overrun can happen if the small switch fails, if it becomes loose from its mounting, or if the change-over relay (described below) gets stuck or fails.
- 5 The three-pole double throw relay is used to change the polarity of the current to the DC motor. Two of the poles carry the motor current, while the third pole is used as holding contacts to keep the relay closed after the microswitch that activated it opens again.
- 6 The two small limit switches are NO and NC. When the NO switch is activated by the cam on the shaft, the relay closes and the polarity to the motor is reversed, changing its direction of rotation. When the switch opens again after a few seconds, the relay stays closed because of the holding contacts described above. The NC limit switch at the other end is wired in series with the holding contacts and the 24V coil. When it is activated by the cam the circuit breaks, the relay opens, and the direction of rotation of the motor is reversed once again.
- 7 The settings of the small limit switches should be set to stop the transverse displacement at the required positions (adjust the cams after releasing the Allen screws).
- 8 The large limit switch should be activated only if one of the small switches is overrun.
- 9 Once overrun, the only way to get it going again will be to override the large limit switch by manually closing the 220V relay (push the button on top). If the direction is not correct, close the 24V relay as well until the mechanism is within its normal working range again.

- 10 It is important to watch the lever arms connected to the gearbox at all times to prevent them from hitting against something solid.
- 11 Also check to see that the transition plate between the curved section of the machine and the pavement at the start of the test pad is not jammed when it moves sideways. Such jamming could possibly occur as a result of the edge left between the worn section of the pavement and the original surface on either side.

